



Chemical Weathering of the Mekong River Basin With Implication for East Asian Monsoon Evolution During the Late Quaternary: Marine Sediment Records in the Southern South China Sea

Pham Nhu Sang^{1*}, Zhifei Liu^{1*} and Christophe Colin²

¹State Key Laboratory of Marine Geology, Tongji University, Shanghai, China, ²GEOPS, CNRS, Université Paris-Saclay, Orsay, France

OPEN ACCESS

Edited by:

Xiting Liu,
Ocean University of China, China

Reviewed by:

Xing Jian,
Xiamen University, China
Upasana Swaroop Banerji,
National Centre for Earth Science
Studies, India

*Correspondence:

Pham Nhu Sang
sang@tongji.edu.cn
Zhifei Liu
lzifei@tongji.edu.cn

Specialty section:

This article was submitted to
Quaternary Science, Geomorphology
and Paleoenvironment,
a section of the journal
Frontiers in Earth Science

Received: 01 March 2022

Accepted: 24 May 2022

Published: 06 July 2022

Citation:

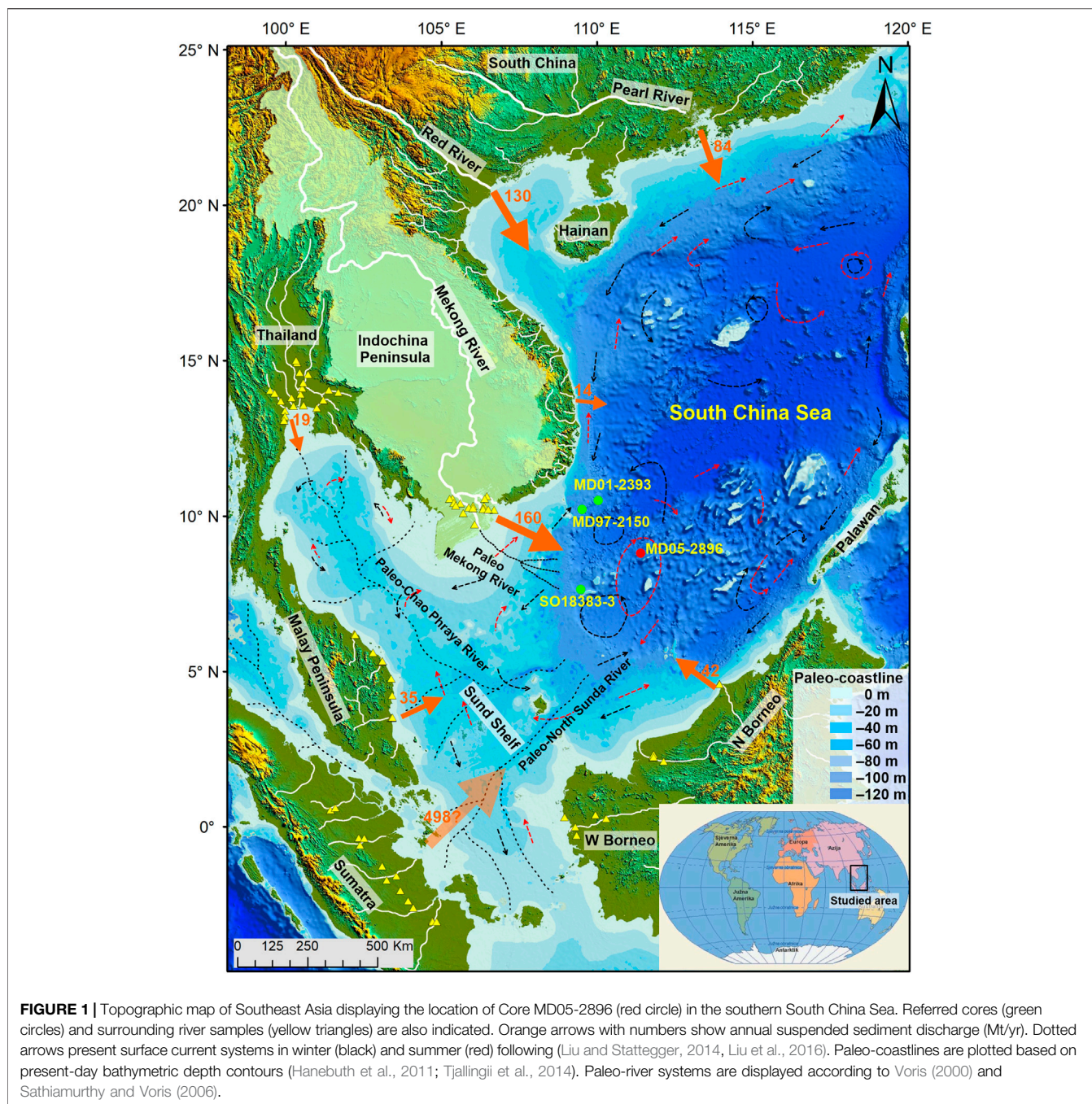
Sang PN, Liu Z and Colin C (2022)
Chemical Weathering of the Mekong
River Basin With Implication for East
Asian Monsoon Evolution During the
Late Quaternary: Marine Sediment
Records in the Southern South
China Sea.
Front. Earth Sci. 10:885547.
doi: 10.3389/feart.2022.885547

Clay mineralogy, major-element geochemistry, and Sr-Nd isotopic compositions from Core MD05-2896 collected in the southern South China Sea have been utilized to investigate the discrimination of sediment provenance and to reconstruct a history of chemical weathering in the Mekong River basin over the last 45 ka. The results display that the clay mineral assemblage of the core is characterized by abundant smectite (27%–56%) and illite (18%–32%), with moderate kaolinite (13%–23%) and chlorite (11%–18%), and the ⁸⁷Sr/⁸⁶Sr ratio and ε_{Nd} value narrowly vary in the ranges of 0.7232–0.7272 and from –10.9 to –9.6, respectively. According to clay mineralogy and Sr-Nd isotopic compositions, the Mekong River is the main terrigenous sedimentary source to the southern South China Sea, with no detectable change over the time span of the study, despite having strong sea-level fluctuations. Clay mineralogy and elemental geochemistry analyses reveal that higher smectite/(illite + chlorite), smectite/kaolinite, TiO₂/K₂O, and SiO₂/K₂O ratios during Marine Isotope Stage (MIS) 3 and 1 suggest enhanced chemical weathering, whereas lower values of these ratios during MIS 2 indicate weakened chemical weathering. These proxies reveal a close relationship with the available climate records of the East Asian monsoon evolution, implying that the chemical weathering in the Mekong River basin has been strongly controlled by the East Asian monsoon rainfall.

Keywords: clay minerals, major elements, Sr-Nd isotopes, chemical weathering, East Asian monsoon, Mekong River, southern South China Sea

1 INTRODUCTION

Chemical weathering of continental rocks is a primary Earth surface process, which significantly relates to atmospheric carbon dioxide consumption and climate change globally (Walker et al., 1981; Berner et al., 1983; Beaulieu et al., 2012). It is a principal influence on global geochemical cycles and provides important materials (i.e., nutrients, elements, etc) from continents to the oceans (Meybeck, 1982; Conley, 2002; Qin et al., 2006). This process on land is mainly controlled by climate conditions, tectonic activity, and lithology (Chamley, 1989; Liu et al., 2007a; Liu et al., 2012), but it is considered a



significant factor responsible for the global climate over the geological timescale (Tamburini et al., 2003; Wan et al., 2007; Clift et al., 2014). Thus, investigation of the weathering process of parent rocks in the source regions and its relationship with monsoon can provide meaningful information in our understanding of the Earth's surface and monsoon evolution (Colin et al., 1999; Wan et al., 2015; Clift et al., 2020).

Marginal sea receives terrigenous sediments from adjacent continents, which contain invaluable information on paleoclimatological and paleoceanographic evolution, making this

region of particular attention to Earth scientists (Yang et al., 2003; Liu and Statterger, 2014; Beny et al., 2018). The South China Sea is the largest marginal sea in the western Pacific, and it has been provided with approximately 700 million tons (Mt) of fluvial sediments annually from numerous surrounding rivers, including three large rivers, namely, the Mekong River (160 Mt/yr), the Red River (130 Mt/yr), and the Pearl River (84 Mt/yr) (Milliman and Syvitski, 1992; Milliman and Farnsworth, 2011) (Figure 1). Terrigenous sediment transport in this region is highly influenced by oceanic circulation, sea-level change, hydrodynamic sorting,

monsoon evolution, and tectonic activities (e.g., Liu et al., 2003; Liu et al., 2007b; Liu et al., 2010; Schimanski and Stattegger, 2005; Clift et al., 2006; Colin et al., 2010; Tjallingii et al., 2010; Tjallingii et al., 2014; Yan et al., 2011; Sang and Liu, 2021). The East Asian monsoon controls seasonal changes in wind patterns, temperature, and rainfall over Southeast Asia, which strongly impact the weathering process on the land, forcing significantly terrigenous sediment variations in the South China Sea (Webster, 1994; Chu and Wang, 2003; Liu et al., 2004; Liu et al., 2005; Chen et al., 2017; Sang et al., 2019). Clay minerals, major elements, and Sr-Nd isotopes are important compositions of terrigenous sediments in this region and contain valuable information on particular characterizations of their source regions and the weathering process on the Earth's surface (Liu and Stattegger, 2014; Liu et al., 2016). These allow them to be widely utilized to identify sediment provenance in the South China Sea and to reconstruct a history of weathering process in the source regions and its relationship to the East Asian monsoon (Clift et al., 2014; Wan et al., 2015; Zhao et al., 2018). The South China Sea, hence, is considered an ideal area in the global marginal seas for investigating East Asian monsoon evolution and paleoceanography (Wang et al., 1995; Wang et al., 1999; Boulay et al., 2007; Liu et al., 2016).

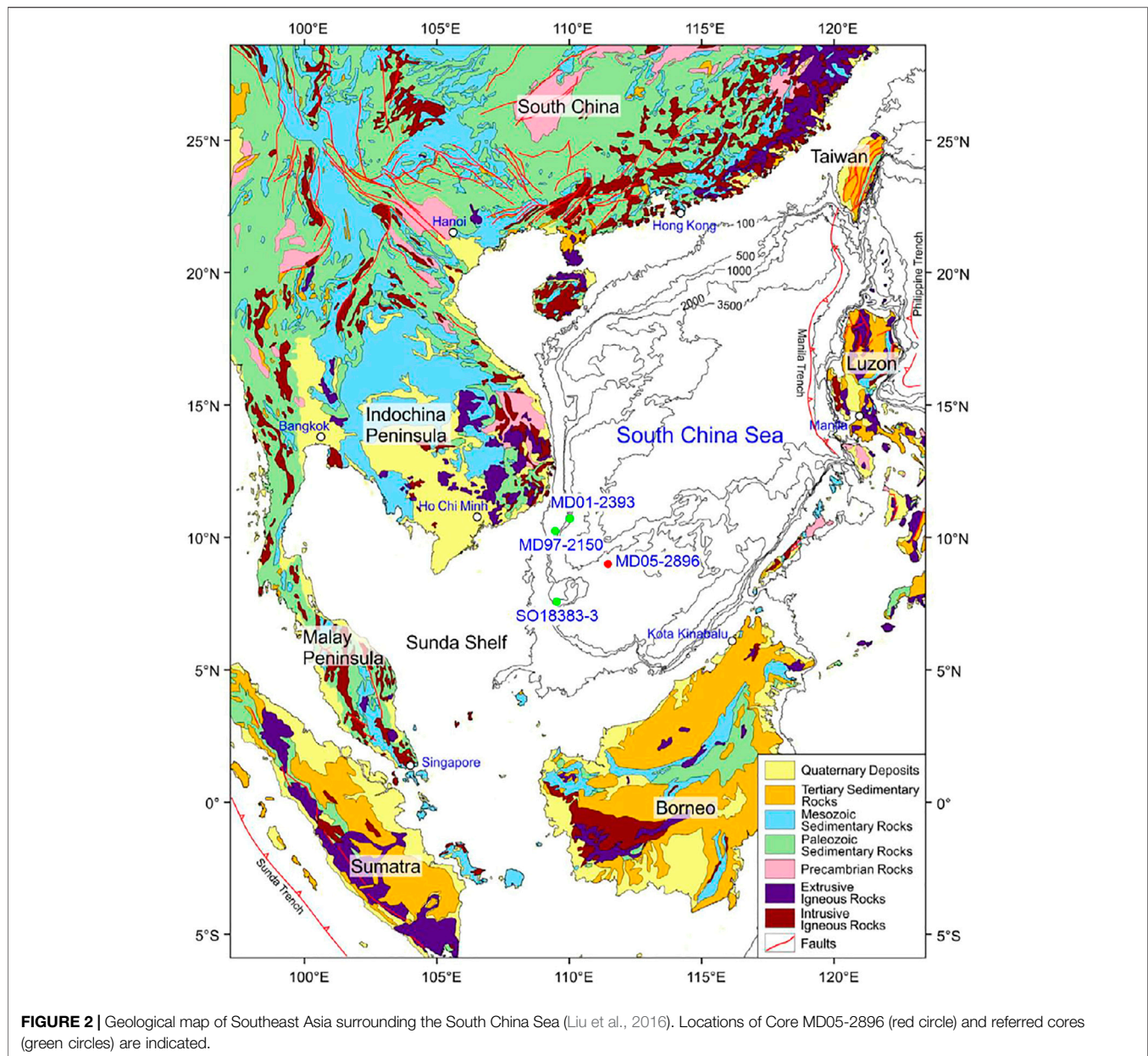
The southern South China Sea inputs huge weathering products of parent rocks from surrounding river basins in Southeast Asia under the strong influence of the East Asian monsoon and sea-level change, and this region becomes a valuable region for studying sediment source-to-sink and land-sea interactions (Hanebuth et al., 2002; Hanebuth et al., 2009; Hanebuth et al., 2011; Steinke et al., 2008; Huang et al., 2016) (Figure 1). Offshore from the Mekong River, clay mineralogy of Cores MD01-2393, MD97-2150 (Liu et al., 2004), and SO18383-3 (Jiwarungrueangkul et al., 2019b) and Sr-Nd isotopic compositions of Core MD01-2393 (Liu et al., 2005) were employed to indicate the Mekong River is the primary source of terrigenous sediments. Liu et al. (2004) and Liu et al. (2005) showed that strengthened chemical weathering corresponds to increased sediment discharge and weakened physical erosion during interglacial periods in the Mekong River basin, whereas weakened chemical weathering is associated with reduced sediment discharge and intensified physical erosion during glacial periods since 190 ka ago. Colin et al. (2010) suggested that higher chemical weathering of detrital material during the Holocene mainly derives from the lower reach of this basin over the last 25 ka. Jiwarungrueangkul et al. (2019b) evaluated moderate chemical weathering in the Mekong River basin since the Last Glacial Maximum. Nevertheless, most of the previous studies offshore from the Mekong River only used clay mineralogy instead of robust proxies (i.e., Sr-Nd isotopic compositions) for identifying bulk terrigenous sediment provenance, and they have not exposed weathering process in the source regions and its relationship with paleoclimate evolution during MIS cycles (i.e., MIS 1, 2, and 3) due to the lack of high-resolution and/or short-term sediment records. Sediment provenance in the southern South China Sea, chemical weathering in the source regions, and its relationship with the East Asian monsoon are, therefore, still not fully understood and require more detailed investigations.

To solve the research questions in the studied area, clay mineralogy, major-element geochemistry, and Sr-Nd isotopic

compositions of Core MD05-2896 in the southern South China Sea are combined to 1) investigate sediment provenance discrimination, especially 2) reconstruct chemical weathering in the source regions and elucidate the relationship between chemical weathering and the East Asian monsoon over the last 45 ka.

2 GEOLOGICAL BACKGROUND

The southern South China Sea is encompassed by the Indochina Peninsula to the west, Borneo to the east, and Sumatra and the Malay Peninsula to the south (Figure 2). In the Indochina Peninsula, the Mekong River flows from the Tibetan Plateau to the South China Sea. The upper reach of this river basin is mainly characterized by Mesozoic sedimentary rocks (meta-sandstone, shale, slate, and phyllite), with minor Precambrian metamorphic and extrusive igneous rocks. The strong physical weathering processes of the parent rocks in this area make high illite and chlorite in lithosols (Liu et al., 2003). Paleozoic–Mesozoic sedimentary rocks (metasandstone, shale, and slate) and intrusive igneous rocks (mainly granites) widely cover the middle reach forming abundantly basaltic and ferrallitic soils. The lithology of the lower reach mainly distributes Mesozoic sedimentary rocks (mostly sandstone and mudstone) with some extrusive igneous rocks (basalts) and a broad alluvial plain primarily with basaltic soils (Segalen, 1995). In Borneo, the lithology consists dominantly of Tertiary sedimentary rocks, with a less abundant distribution of Paleozoic–Mesozoic sedimentary rocks in the central part, of Paleozoic–Mesozoic granite and granodiorite and Tertiary volcanic rocks in the southwestern part, and of Quaternary sediments in the coastal plain and delta (Figure 2). The sedimentary rocks contain mostly sandy shale, partly interbedded with coal beds, sandstone, and carbonate rocks (Hutchison, 2005). Sparse Tertiary basic volcanic rocks and Mesozoic basic–ultrabasic intrusive rocks are mainly distributed in central tectonic belts. Borneo has been tectonically active throughout the Cenozoic and displayed the strongest tectonic uplift during the Oligocene–Miocene period (Hall, 2002; Hutchison, 2005). Sumatra consists mainly of Quaternary intermediate to basic volcanic rocks in the mountains and slopes of the southwest and late Tertiary sedimentary rocks in the northwest, with a minor distribution of Quaternary sediments along rivers and coastline (Liu et al., 2012) (Figure 2). Besides, this region is covered sparsely by Paleozoic–Mesozoic volcanic, intrusive, and sedimentary rocks and Tertiary basalts. This area has been forced by northeastward subduction of the Indian Ocean Plate along the Sunda Trench in the eastern Indian Ocean and the Sumatra strike-slip fault on the mountainous range of the southwestern island (Barber and Crow, 2009), causing highly tectonically active since the Tertiary. Sumatra shows an extremely active volcanic eruption history with the abundant distribution of Quaternary basic–intermediate volcanic rocks. The Malay Peninsula occurs abundantly in Paleozoic–Mesozoic granite and granodiorite and Paleozoic sedimentary rocks, with minor Mesozoic (mainly Jurassic–Cretaceous) sedimentary rocks and sparse basic volcanic rocks (Liu et al., 2012) (Figure 2). Quaternary sediments have been distributed primarily along the coastline. Mudstone, sandstone, and limestone, interbedded with andesitic–rhyolitic volcanic rocks are the



main compositions of the sedimentary rocks (Hutchison, 2005; Sultan and Shazili, 2009). This Peninsula has displayed stable tectonic activities since the Mesozoic period (Hutchison, 1968).

3 MATERIALS AND METHODS

3.1 Materials

Core MD05-2896 ($8^{\circ}49.5'N$, $111^{\circ}26.47'E$; 1,657 m water depth; 11.03 m long) was collected in the southern South China Sea during the cruise of MARCO POLO in 2005 (Laj et al., 2005) (Figure 1). The upper 4.69 m of this core was used for the present study wherein the samples were collected at 4 cm intervals from surface to 3.13 m whereas from 3.13 to 4.69 m the core was

sampled at 2 cm intervals. A total of 178 samples were collected for clay mineralogy and major-element geochemistry analyses. Twelve of these samples were chosen to measure Strontium (Sr) and Neodymium (Nd) isotopic compositions. The age model was established by using planktonic foraminiferal AMS ^{14}C dating and benthic foraminiferal $\delta^{18}O$ records (Wan and Jian, 2014; Wan et al., 2020). All these analyses were performed at the State Key Laboratory of Marine Geology, Tongji University.

3.2 Analytical Methods

Clay minerals were identified by X-ray diffraction (XRD) using a PANalytical X'Pert PRO diffractometer on oriented mounts of non-calcareous clay-sized ($<2\mu m$) particles (Holtzapffel, 1985). The carbonate of sediment samples was removed by using 0.2 N HCl.

The oriented mounts were prepared following the methods described in Liu et al. (2004). Three XRD runs were performed following pretreatment conditions of air drying, ethylene-glycol solvation for 24 h, and heating at 490°C for 2 h. To identify clay minerals, the position of the (001) series of basal reflections on the three XRD diagrams was employed. Based on the glycolated curve, the MacDiff software was used to determine semiquantitative estimates of peak areas of the basal reflections for the main clay mineral groups of smectite, including mixed-layer minerals (15–17 Å), illite (10 Å), and kaolinite/chlorite (7 Å) (Holtzapffel, 1985; Petschick, 2000). Relative proportions of kaolinite and chlorite were identified using the ratios of the 3.57/3.54 Å peak areas. Furthermore, some mineralogical characteristics of illite were identified on the glycolated curve. The illite chemistry index was calculated utilizing the ratio of the 5 Å and 10 Å illite peak areas in glycol-saturated samples (Esquevin, 1969). Ratios below 0.5 represent Fe–Mg-rich illite (biotite, mica) characterized by physical erosion; ratios above 0.5 are mainly found in Al-rich illite (muscovite) formed by strong hydrolysis (Esquevin, 1969; Gingele et al., 1998). Illite crystallinity was estimated with full width at half maximum of illite 10 Å peak. Lower values represent the higher crystallinity and indicate weak hydrolysis in continental sources and arid and cold climate conditions (Chamley, 1989; Krumm and Buggisch, 1991; Ehrmann, 1998).

Major elements were measured on fused glass by X-ray fluorescence (XRF) using a PANalytical Axios^{MAX} spectrometer. The samples were first reacted with 0.2 N HCl to remove carbonate and then dried under 60°C. The decarbonated samples were fused and analyzed by the XRF method to obtain major element concentrations. The glass beads were prepared using ~0.7000 g of sediment sample combined with ~7.000 g of Li₂B₄O₇. Chinese rock and sediment standards GRS02 and GRS04 were used to monitor the analytical precision and accuracy. Major elements were expressed as their oxides as absolute bulk contents of samples after carbonate removal. Considering the objectives of terrigenous clastic compositions of this study, total organic carbon (TOC) and total inorganic carbon (TIC) as well as the loss of ignition (LOI) were not measured separately prior to the fusion because the data were not planned for usage. However, given the fusion method of our XRF analysis, the LOI values can be roughly calculated by subtracting all the major elements from 100%. All these data are included in the **Supplementary Material**.

Sr and Nd isotopic compositions of bulk carbonate-free terrigenous sediments were analyzed using a Thermo Scientific Neptune Plus MC-ICP-MS. Geostandards GSR-6 and GSD-9 were used to monitor the precision and accuracy. A small subsample of the sediment samples was dried at low temperature (~50°C) and crushed to a fine powder. The powder samples were treated with 1 N HCl to remove calcium carbonate and authigenic components. They were then heated at 600°C for 2 h to remove the organic carbon. A ~50 mg of each sample was totally digested with a mixture of concentrated HF and HNO₃ in high-pressure Teflon bombs at 190°C for at least 48 h. Sr and Nd were separated following the procedure described in detail by Wu et al. (2021). Sr and Nd isotopic compositions were normalized to $^{86}\text{Sr}/^{88}\text{Sr} = 0.1194$ and $^{146}\text{Nd}/^{144}\text{Nd} = 0.7219$, respectively. The standards SRM987 ($^{87}\text{Sr}/^{86}\text{Sr} = 0.710250 \pm 0.000016$, Lugmair et al., 1983) and JNdi-1 ($^{143}\text{Nd}/$

$^{144}\text{Nd} = 0.512115 \pm 0.000006$, Tanaka et al., 2000) were used to monitor the quality of $^{87}\text{Sr}/^{86}\text{Sr}$ and $^{143}\text{Nd}/^{144}\text{Nd}$, respectively. The mean measured $^{87}\text{Sr}/^{86}\text{Sr}$ value of SRM987 was 0.710242 ± 12 (2σ , $N = 10$), and the mean measured $^{143}\text{Nd}/^{144}\text{Nd}$ of JNdi-1 was 0.512118 ± 8 (2σ , $N = 10$), well within the recommended values. Nd isotopic data are expressed as $\epsilon_{\text{Nd}} = [({}^{143}\text{Nd}/{}^{144}\text{Nd})_{\text{measured}}/({}^{143}\text{Nd}/{}^{144}\text{Nd})_{\text{CHUR}} - 1] \times 10^4$. The CHUR (Chondritic Uniform Reservoir) value is 0.512638 (Jacobsen and Wasserburg, 1980).

4 RESULTS

4.1 Clay Minerals

The clay mineral assemblage of Core MD05-2896 consists of dominant smectite (27%–56%) and illite (18%–32%), with moderate kaolinite (13%–23%) and chlorite (11%–18%) (**Figure 3**). All these clay minerals present high variability over the past 45 ka; however, their variability can be distinguished between MIS 3, 2, and 1. Kaolinite, illite, and chlorite contents exhibit a similar pattern with decreased values during MIS 3 and 1, and increased values during MIS 2. On the contrary, smectite content displays an inverse pattern with high values during MIS 3 and 1 and low values during MIS 2. Illite crystallinity and illite chemistry index show high variations in values between 0.16 and $0.22^\circ\Delta 2\theta$ (average $0.19^\circ\Delta 2\theta$) and from 0.39 to 0.59 (average 0.45), respectively, and they display no visible trend over the last 45 ka.

4.2 Major Elements

In Core MD05-2896, the major elements contain dominant SiO₂, Al₂O₃, and Fe₂O₃ (in total ~84%), with minor K₂O, MgO, TiO₂, Na₂O, CaO, MnO, and P₂O₅ (~7% in total) (**Figure 4**). Generally, variations in Al₂O₃, Fe₂O₃, K₂O, and Na₂O contents present inverse correlations to those of TiO₂, SiO₂, and MgO contents over the last 45 ka. Al₂O₃, Fe₂O₃, K₂O, and Na₂O contents display increased values during MIS 3 and 2, and decreased values during MIS 1. In contrast, TiO₂, SiO₂, and MgO contents are characterized by low values during MIS 3 and 2, and high values during MIS 1. Nevertheless, P₂O₅ content exhibits little variation in values with no obvious trend during MIS 3, 2, and 1. CaO content shows high values during MIS 3 and decreased values after late MIS 3 to the present time.

4.3 Sr-Nd Isotopes

$^{87}\text{Sr}/^{86}\text{Sr}$ ratios of terrigenous sediments from Core MD05-2896 vary between 0.7232 and 0.7272, and ϵ_{Nd} values range from –10.9 to –9.6 (**Figure 3**; **Table 1**). Downcore variations in $^{87}\text{Sr}/^{86}\text{Sr}$ ratios increase in values from MIS 3 to MIS 1, and ϵ_{Nd} shows increased values from MIS 3 to middle MIS 2 and decreased values after middle MIS 2 to the present time.

5 DISCUSSION

5.1 Sediment Provenance Discrimination

Generally, ways of transportation, weathering processes in source regions, and sea-level change can induce variability of clay mineral assemblage and Sr-Nd isotopic compositions of Core

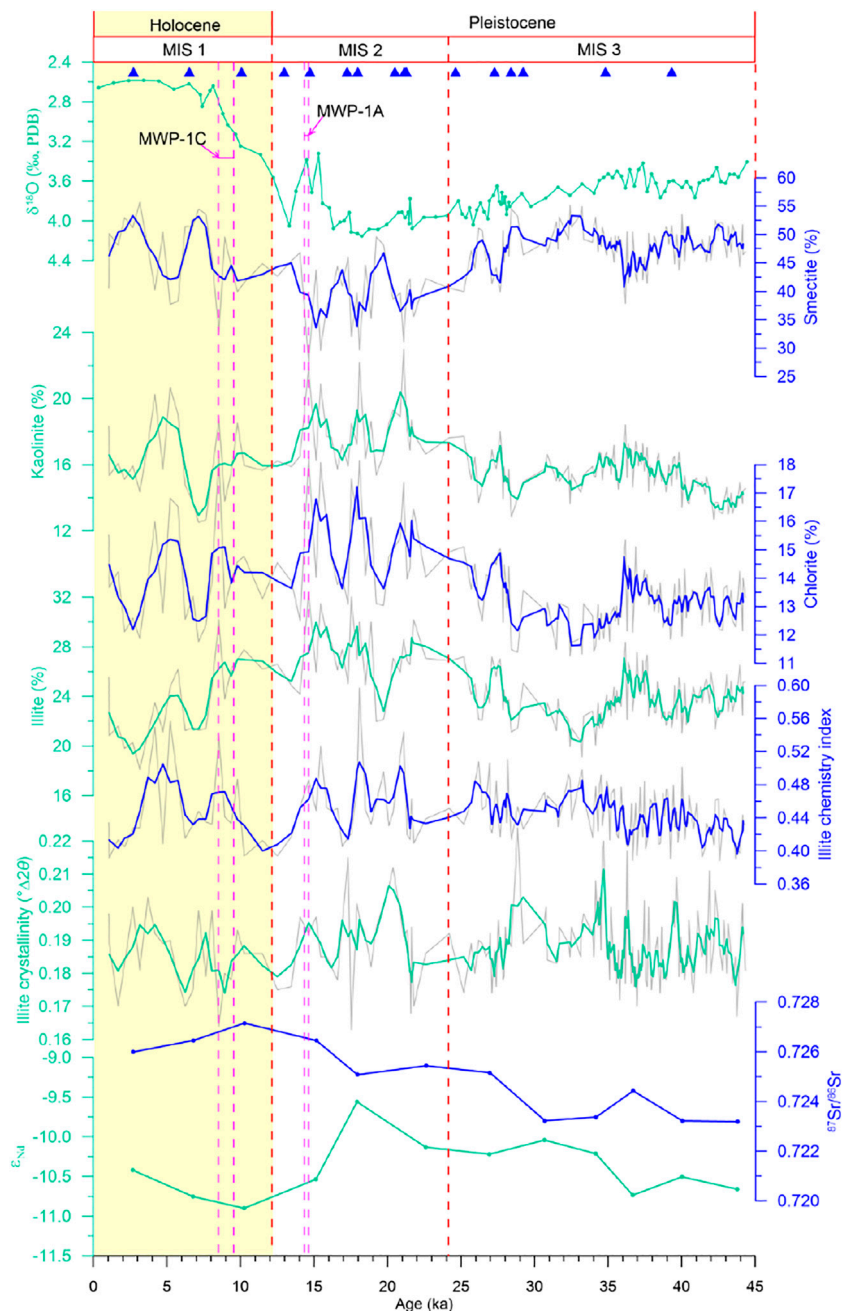


FIGURE 3 | Temporal variations of clay mineral assemblage and Sr-Nd isotopic values of Core MD05-2896 over the last 45 ka. The benthic foraminiferal *C. wuellerstorfi* $\delta^{18}\text{O}$ stratigraphy and foraminiferal AMS ^{14}C datings (blue triangle) (Wan and Jian, 2014; Wan et al., 2020) are also displayed. Dashed magenta lines indicate the meltwater pulses 1A (MWP-1A) (Hanebuth et al., 2000) and 1C (MWP-1C) (Tjallingii et al., 2010). MIS 1 (0–12.05 ka), MIS 2 (12.05–24.11 ka), and MIS 3 (24.11–45.00 ka) display marine isotope stages (Martinson et al., 1987). The clay mineral data were smoothed by a three-point running average (coarse).

MD05-2896. Clay mineral assemblages and Sr-Nd isotopic compositions of marine sediments have been then extensively utilized to elucidate potential sediment provenance (Clift et al., 2002; Liu et al., 2008; Lupker et al., 2013; Cai et al., 2020), resulting in tracking sediment transport in the sea (Liu et al., 2007b; Liu et al., 2010; Zhao et al., 2018). Terrigenous sediments in the southern South China Sea derive mainly from the

surrounding rivers, such as the Mekong River and small rivers from Borneo (42 Mt/yr), Sumatra (498 Mt/yr, model data), the Malay Peninsula (35 Mt/yr), and Thailand (19 Mt/yr) (Figure 1) due to the trivial contribution of eolian fluxes in this region (Wehausen et al., 2003). The small mountainous rivers in central Vietnam mainly provide huge terrigenous sediments to the central Vietnam shelf (Schimanski and Statterger 2005; Sang

TABLE 1 | Sr and Nd isotopic compositions of Core MD05-2896 over the last 45 ka.

No.	Depth (cm)	Age (ka)	$^{87}\text{Sr}/^{86}\text{Sr}$	$\pm 2\sigma$	$^{143}\text{Nd}/^{144}\text{Nd}$	$\pm 2\sigma$	ϵ_{Nd}	$\pm 2\sigma$
1	19	2.68	0.725989	0.000016	0.512104	0.000006	-10.42	0.12
2	51	6.77	0.726454	0.000013	0.512087	0.000008	-10.75	0.15
3	83	10.24	0.727152	0.000017	0.512079	0.000007	-10.90	0.14
4	107	15.13	0.726448	0.000013	0.512098	0.000007	-10.53	0.14
5	139	17.92	0.725081	0.000018	0.512148	0.000009	-9.56	0.18
6	199	22.59	0.725440	0.000015	0.512119	0.000011	-10.13	0.21
7	243	26.93	0.725164	0.000014	0.512114	0.000008	-10.22	0.15
8	313	30.67	0.723227	0.000017	0.512123	0.000008	-10.04	0.16
9	331	34.15	0.723374	0.000019	0.512115	0.000012	-10.21	0.23
10	365	36.67	0.724428	0.000016	0.512088	0.000011	-10.73	0.21
11	410	40.02	0.723218	0.000015	0.512100	0.000009	-10.50	0.18
12	461	43.76	0.723193	0.000015	0.512092	0.000009	-10.66	0.18

et al., 2019), whereas they contribute a minor volume of terrigenous fine detrital materials to the western South China Sea (Liu et al., 2007b) and offshore from the Mekong River (Liu et al., 2004; Liu et al., 2005). Hence, terrigenous sediment contributions from these rivers in central Vietnam will not be discussed more thereafter.

5.1.1 Evidence From Clay Minerals

To determine the provenance of clay minerals in the region during the late Quaternary, all clay mineral samples of Core MD05-2896 are grouped into two intervals: Holocene and Pleistocene samples. The proportion of kaolinite, illite + chlorite, and smectite at this core is compared to the potential sources mentioned above and referred to as Cores SO18383-3, MD01-2393, and MD97-2150 offshore from the Mekong River, respectively (Figure 5). Clay mineral assemblage of Core MD05-2896 in comparison with the potential sediment sources shows that clay minerals in this region may originate from multiple sources due to no distinct overlap (e.g., Liu et al., 2007b; Steinke et al., 2008; Wang et al., 2015; Chen et al., 2017; Zhao et al., 2018). However, some robust evidence below indicates that the Mekong River can provide mainly clay minerals to this studied area. Clay mineral assemblages of Holocene and Pleistocene samples at Core MD05-2896 are overlaid, indicating no major changes in clay mineral sources during the late Quaternary. Additionally, the clay mineral assemblage of Core MD05-2896 and the referred cores are situated nearly each other, implying that these cores can have the same source of clay minerals. According to Liu et al. (2004) and Jiwaringrueangkul et al. (2019b), clay minerals of Cores MD01-2393, MD97-2150, and SO18383-3 primarily come from the Mekong River, suggesting that this river can be the most crucial source of clay minerals at Core MD05-2896 as well.

Illite and chlorite are mainly formed by the physical erosion processes in the source regions under cold and arid climatic conditions (Chamley, 1989). Furthermore, illite and chlorite at Core MD05-2896 display a similar pattern over the last 45 ka (Figure 3). Based on their formation in the source regions and patterns during MIS 3, 2, and 1, illite and chlorite are generally similar to sediment sources (e.g., Liu et al., 2007b; Liu et al., 2008). Surrounding the southern South China Sea, the Mekong River and rivers in North Borneo are characterized by high illite

(average 35% and 56%, respectively) and chlorite (average 26% and 25%, respectively) in sediments (Liu et al., 2007a; Liu et al., 2012). In North Borneo, strong physical erosion of parent rocks has been caused by active tectonic setting since the Mesozoic and especially the rapid uplift during the Oligocene-Miocene (Rangin et al., 1990; Hutchison, 2005) (Figure 2) and the abundant seasonal precipitation (Liu et al., 2012), yielding high illite and chlorite in river sediments. In the Mekong River basin, metamorphic and granitic parent rocks extensively occur in the eastern Tibetan Plateau under cold and dry climate conditions where illite and chlorite can be produced highly in weathering products (Liu et al., 2004) (Figure 2). Nevertheless, this studied area can receive primarily illite and chlorite from the Mekong River, with negligible contributions from rivers in North Borneo due to some probable evidence. First, rivers in North Borneo are characterized by small drainage areas, short length, and no significant sediment discharge, implying that they cannot contribute an essential amount of terrigenous sediments to this region (Figure 1). In contrast, the Mekong River drains a large catchment of 790,000 km², supplying the highest amounts of terrigenous sediments to the southern South China Sea. Additionally, this river mouth is much closer to the location of Core MD05-2896 than those of rivers in North Borneo. These suggest a higher contribution from the Mekong River compared to rivers in North Borneo. Second, the illite chemistry index and illite crystallinity of marine sediments have been extensively employed to trace the source of illite in the South China Sea (Liu et al., 2007b; Liu et al., 2008; Liu et al., 2016; Jiwaringrueangkul et al., 2019a; Sang et al., 2019). Illite chemical index and illite crystallinity are determined by the type and intensity of weathering in river basins (Chamley, 1989), but they show no obvious trends between MIS 1, 2, and 3 in this study (Figure 3), implying significant relation to the source of illite instead of the chemical weathering process in the source regions. To elucidate a vital source of illite in this region, the illite chemistry index and illite crystallinity of Core MD05-2896 are plotted compared with those of referred Cores MD01-2393, MD97-2150, and SO18383-3 and potential sources (Figure 6). Most of the samples at Core MD05-2896 are close to the Mekong River samples, while they display long distances with other potential sources, especially rivers in North and West

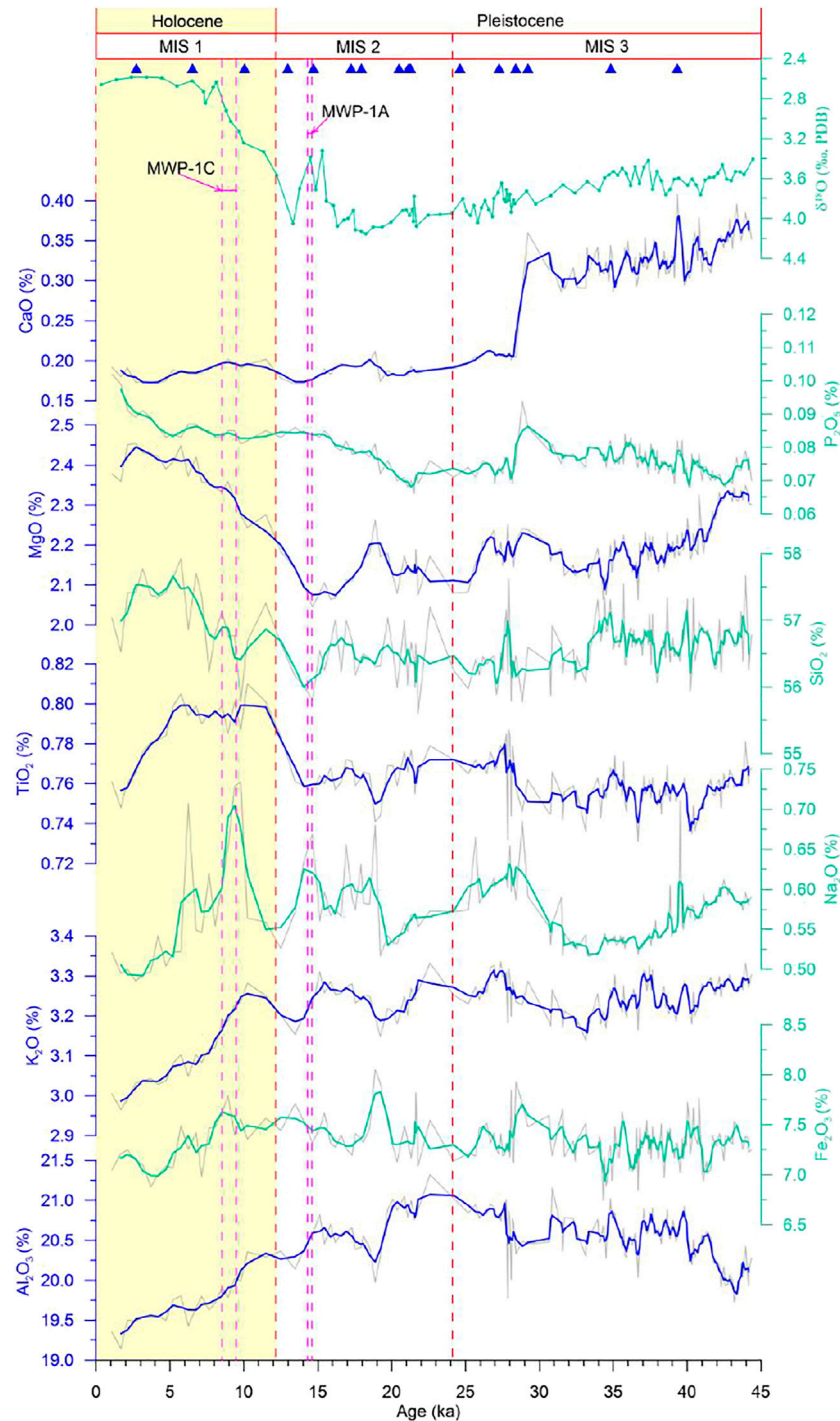
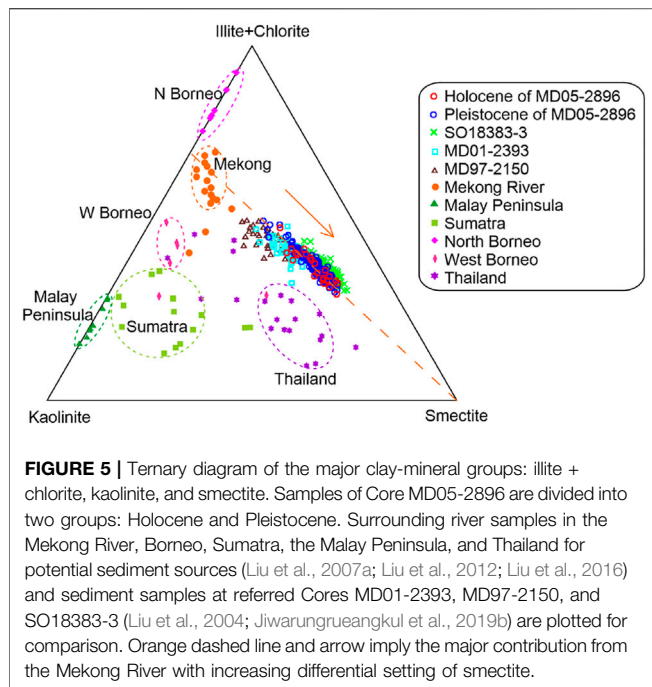


FIGURE 4 | Temporal variations of major elements of Core MD05-2896 over the last 45 ka. The benthic foraminiferal *C. wuellerstorfi* $\delta^{18}\text{O}$ stratigraphy and foraminiferal AMS ^{14}C datings (blue triangle) (Wan and Jian, 2014; Wan et al., 2020) are also displayed. Dashed magenta lines indicate the meltwater pulses 1A (MWP-1A) (Hanebuth et al., 2000) and 1C (MWP-1C) (Tjallingii et al., 2010). The major element data were smoothed by a three-point running average (coarse).

Borneo. Additionally, illite at Cores MD01-2393, MD97-2150, and SO18383-3 is provided chiefly by the Mekong River (Liu et al., 2004; Jiwarungrueangkul et al., 2019b), but their samples

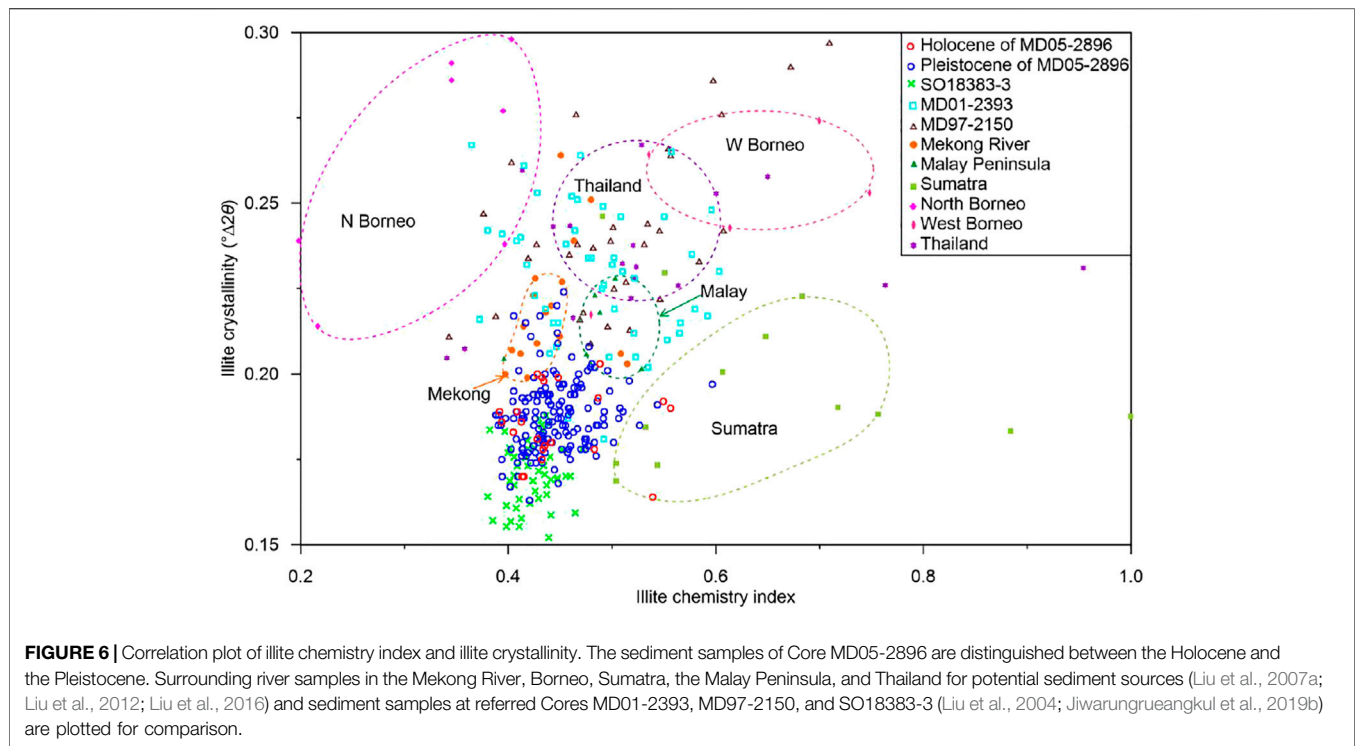
are less close to the Mekong River samples than those of Core MD05-2896. The Mekong River is, therefore, the most significant source of illite and chlorite in the studied region.



The formation of kaolinite usually relates to monosalitization of parent rocks, characterizing intensive chemical weathering (Chamley, 1989). Kaolinite is easily formed by parent rocks enriched in alkali and alkaline elements (e.g., granite, granodiorite, and intermediate-acid volcanic rocks) under warm and humid climates. In the potential source regions, kaolinite abundantly occurs in river sediments from the Malay Peninsula (average 80%), Sumatra (average 57%), West Borneo (average 47%), Thailand (average 32%), and the Mekong River (average 28%) (Liu et al., 2007a; Liu et al., 2012). However, the Mekong River can be the most important potential source of kaolinite at Core MD05-2896 (average 16%) due to its location and sediment discharge, as well as the differential setting tendency of kaolinite in saline water. Paleozoic-Mesozoic sedimentary rocks (i.e., mudstone, sandstone, and limestone, interbed with andesitic-rhyolitic volcanic rocks) and Paleozoic-Mesozoic granite and granodiorite rocks in the Malay Peninsula easily form kaolinite under warm and humid East Asian-Australian monsoon climate and stable tectonics since the Mesozoic (Hutchison, 1968; Sultan and Shazili, 2009; Liu et al., 2012) (Figure 2). In Sumatra, the majority of Quaternary intermediate-basic volcanic rocks highly yield kaolinite in weathering products under the strong influence of the monsoon climate with the warm temperature and dominant precipitation because of the well-developed monosalitization (Liu et al., 2012) (Figure 2). The monosalitization of intrusive and volcanic rocks in West Borneo produces high kaolinite in river sediments under the warm and humid monsoon climate. In Thailand, parent rocks mainly contain granite, granodiorite, and intermediate-acid and basic volcanic rocks, which are undergone warm and humid climate conditions, producing high kaolinite in river sediments (Liu et al., 2016) (Figure 2). However, kaolinite tends to deposit close to its sources because it is a relatively large

size (0.5–8.0 μm in diameter) and strongly flocculated in alkaline seawater (Gibbs, 1977; Johnson and Kelley, 1984; Patchineelam and Figueiredo, 2000). As a consequence, kaolinite is distributed highly in sediments from surrounding fluvial systems in the South China Sea (i.e., the Malay Peninsula, South China, central Vietnam, and West Borneo) (Liu et al., 2016), implying that kaolinite in this area can come mainly from proximal sources (i.e., the Mekong River) instead of remote sources (i.e., rivers in Borneo, Sumatra, the Malay Peninsula, and Thailand) (Figure 1). The Mekong River mouth is much closer to Core MD05-2896 and displays much higher terrigenous sediment contribution than those of other small rivers surrounding the southern South China Sea. Furthermore, more kaolinite in the Malay Peninsula, Sumatra, Thailand, and West Borneo should be supplied to the region during the Holocene because of increased southwesterly summer monsoon currents. Nevertheless, kaolinite displays lower content during the Holocene than during glacial MIS 2. Therefore, rivers in Sumatra, the Malay Peninsula, West Borneo, and Thailand can contribute kaolinite insignificantly to the studied site. It is then reasonable to conclude that the Mekong River is the main source of kaolinite transported to the Core MD05-2896. Variations of kaolinite proportions display a good positive correlation with those of illite and chlorite (Figure 3). This suggests that all these clay minerals derive from physical erosion processes of different parts of the Mekong River basin. According to Liu et al. (2004), kaolinite could originate from active erosion of inherited clays of ferrallitic soils in a lower part of the middle reach in the Mekong River basin. Additionally, kaolinite can be transported by reworking from the exposed continental shelf during the sea-level low-stand.

Smectite may be formed by the chemical weathering of volcanic rocks in the source regions, which contains basic materials such as Fe-Mg species and rhyolitic materials under warm and humid climate conditions (Chamley, 1989). Smectite is dominant in rivers from Thailand (average 42%), moderate in Sumatra rivers (average 19%), and low in West Borneo rivers (average 14%) and the Mekong River (average 11%) (Liu et al., 2007a; Liu et al., 2012). Nevertheless, the Mekong River emerges to play the most critical role in providing smectite to this studied area. Smectite displays the highest content in river sediments from Thailand due to the abundant basaltic lithology in these drainage systems under hot-warm climate conditions (Figure 2). However, rivers in Thailand do not yield much terrigenous sediments to the sea annually, and most of the terrigenous sediments are trapped within the Gulf of Thailand, and little exchange of clay minerals happens between gulf of Thailand and the southern South China Sea because of the strong clockwise surface circulation in the entrance region during the Holocene (Liu et al., 2016) (Figure 1). These imply that smectite in the region could not come mainly from rivers in Thailand. In Sumatra, the majority of Quaternary intermediate-basic volcanic rocks are considered potential parent rocks for producing moderate smectite in river sediments (Liu et al., 2012) (Figure 2). Furthermore, the occurrence of basic Tertiary volcanic rocks in West Borneo can produce smectite in river sediments, too, but these rivers contribute only minor terrigenous sediments to the sea. Kaolinite shows dominant contents in river sediments in Sumatra and West



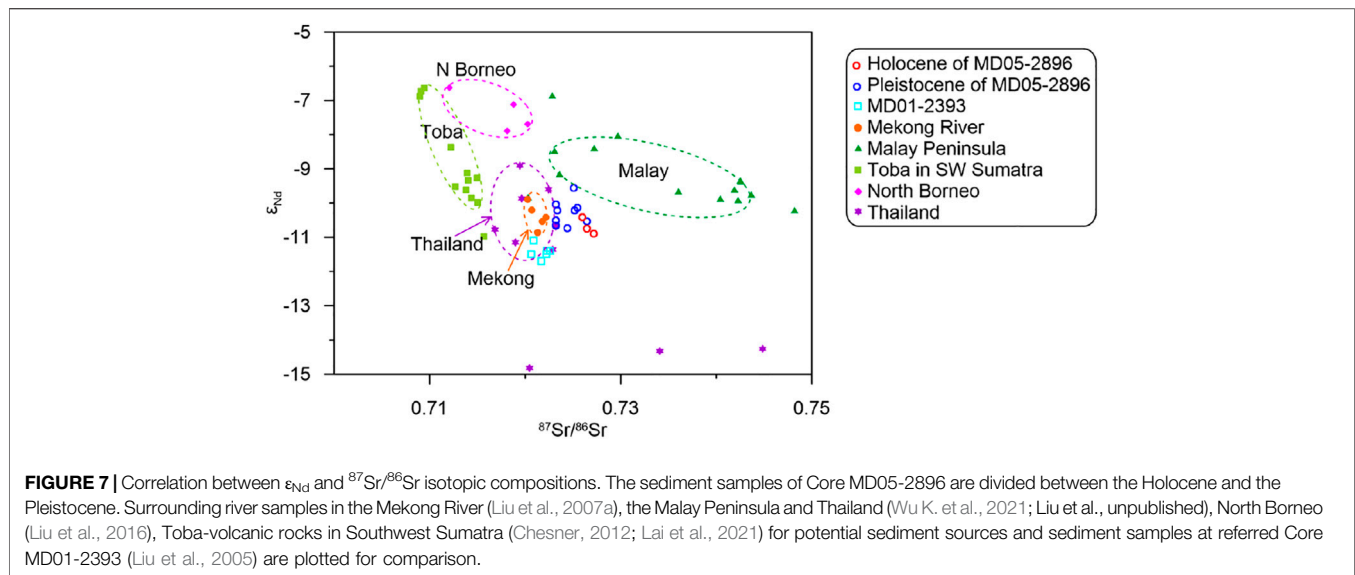
Borneo, but the increase of smectite is not associated with the increase of kaolinite (Figure 3). Additionally, the temperature is mostly stable in the tropical region (Warrier and Shankar 2009), and the winter monsoon primarily supplies the precipitation in tropical lands surrounding the southern South China Sea, implying that the enhanced winter monsoon may bring much more precipitation to those regions (Sun et al., 2002; Hu et al., 2003; Wang et al., 2009). These climatic conditions allow parent rocks in these tropical regions to produce more smectite in weathering products during the last glacial period. Nevertheless, smectite at Core MD05-2896 displays lower values during the last glacial period (MIS 2) than during the Holocene (MIS 1) (Figure 3). These suggest that rivers in Sumatra and West Borneo cannot provide a valuable amount of smectite to this region. Therefore, rivers in Thailand, Sumatra, and West Borneo can transport only negligible amounts of smectite to the studied area, and smectite at Core MD05-2896 mainly originates from the Mekong River. Sediments in the Mekong River are characterized by low smectite, but this river can be sufficiently a source for smectite of Core MD05-2896 due to the close relationship between the differential setting effect of smectite in more saline and distal waters and the South China Sea basin-wide clay mineral distribution (Liu et al., 2016). Smectite in this region can be weathering products of parent aluminosilicate and ferromagnesian silicates in the middle to lower reaches of the Mekong River under warm and humid climate conditions (Liu et al., 2004) (Figure 2).

5.1.2 Evidence From Sr-Nd Isotopes

Bulk terrigenous sediments of Core MD05-2896 display high $^{87}\text{Sr}/^{86}\text{Sr}$ ratios and low ϵ_{Nd} values (Table 1), indicating that terrigenous sediments in this region can come mainly from old continental materials. Sr-Nd isotopic compositions in weathering products

depend on crustal domains and tectonic backgrounds (McLennan et al., 1990; McLennan and Hemming, 1992). Nd is more immobile than Sr during chemical weathering, suggesting that Nd can be enriched in weathering products, whereas Sr will be removed easily from parent rocks during chemical weathering. In addition, ϵ_{Nd} values and $^{87}\text{Sr}/^{86}\text{Sr}$ ratios can be influenced by size fractions of the sediments, as decreased grain size of sediments can cause increased $^{87}\text{Sr}/^{86}\text{Sr}$ ratios, and ϵ_{Nd} will be more radiogenic (Revel et al., 1996; Innocent and Fagel, 2000). Naturally, variations in Sr-Nd isotopic compositions of terrigenous sediments at Core MD05-2896 may depend on intensive chemical weathering and grain size fractions, but they are still helpful for tracing sediment provenance (e.g., Walter et al., 2000; Colin et al., 2006; Wei et al., 2012; Lupker et al., 2013; Wan et al., 2015; Wan et al., 2017).

To elucidate the terrigenous sediment provenance, Holocene and Pleistocene Sr-Nd isotopic compositions of Core MD05-2896 are plotted to compare with those of the potential sources and referred to Core MD01-2393 (Figure 7). Surrounding this region, $^{87}\text{Sr}/^{86}\text{Sr}$ ratios and ϵ_{Nd} values of the Mekong River and rivers in Thailand are much close to those of Core MD05-2896 and surface sediments of these rivers are mainly weathering products of old continental materials. Taking into consideration the short distance of the Mekong mouth to the studied site and the huge sediment discharge of the Mekong River, we can hypothesize that the Mekong River is the main sedimentary source. Although $^{87}\text{Sr}/^{86}\text{Sr}$ ratios and ϵ_{Nd} values of river sediments from Thailand also are quite close to those of the cores, these rivers can contribute insignificantly terrigenous sediments to the sea and their remote locations (Figure 1). Additionally, if rivers in Thailand would supply crucial amounts of terrigenous sediments to the region, rivers in the Malay Peninsula and Sumatra can also transport much fluvial



sediments to this studied area. Nevertheless, rivers from the Malay Peninsula and Toba-volcanic rocks in southwestern Sumatra clearly show much different $^{87}Sr/^{86}Sr$ ratios and ϵ_{Nd} values compared with those of the core. This suggests that rivers from these areas cannot be important sources of terrigenous sediments to the Core MD05-2896. As a result, rivers in Thailand cannot transport a significant amount of terrigenous sediments to the studied area. In addition, river sediments from North Borneo and these cores also differ in $^{87}Sr/^{86}Sr$ ratios and ϵ_{Nd} values, suggesting terrigenous sediments offshore from the Mekong River cannot come significantly from rivers in North Borneo as well. As illustrated in **Figure 7**, the $^{87}Sr/^{86}Sr$ ratios and ϵ_{Nd} values of Cores MD05-2896 and MD01-2393 are adjacent to each other, determining that these cores originate from the same source. Provenance analysis based on Sr-Nd isotopic compositions of Core MD01-2393 indicated that the Mekong River is considered the primary source of this core (Liu et al., 2005), suggesting this river also provides mainly terrigenous sediments of Core MD05-2896. The $^{87}Sr/^{86}Sr$ ratios and ϵ_{Nd} values of the Holocene and Pleistocene samples of both cores are imbricated clearly, suggesting no change in terrigenous sediment sources since the late Pleistocene. Consequently, the Mekong River emerges as the most important source contributing bulk terrigenous sediments to the southern South China Sea without significant change in sediment sources during the late Quaternary. Furthermore, ϵ_{Nd} shows little higher values during MIS 2 than MIS 3 and 1, implying that stronger physical weathering of parent rocks with more positive Nd isotopes in the eastern Tibetan Plateau during MIS 2 can provide more terrigenous sediments from the highland part to the Core MD05-2896. This hypothesis is consistent with provenance analysis based on clay mineralogy above, implying bulk and clay-fraction sediments are the same source and mainly originate from the Mekong River.

5.2 Effect of Sea-Level Change

Generally, global sea-level change can impact coastline configuration (i.e., location of estuary system) and offshore sediment transport concerning river power and marine forcing, causing sediment source changes and/or variations in terrigenous sediment discharge.

Terrigenous sediment input to the southern South China Sea off the Sunda Shelf can be influenced strongly by sea-level changes (Steinke et al., 2008; Huang et al., 2016; Jiwarungrueangkul et al., 2019a), whereas the terrigenous sediment variations offshore from the Mekong River should be less sensitive to sea-level fluctuations. In this region, the significant sea-level rise was as much as 16 m from 14.6 to 14.3 ka at the meltwater pulse 1A (MWP-1A) (Hanebuth et al., 2000) (**Figure 8**), forming a rapid retreat of the Paleo-Chao Phraya River mouth toward the land, whereas there is no important change in the location of the Paleo-Mekong River estuary (Voris, 2000; Sathiamurthy and Voris, 2006) (**Figure 1**). This is due to the continental shelf at the Paleo-Mekong River mouth being characterized by a high gradient and not by large morphology (Tjallingii et al., 2010), making this paleo-river retreat insignificantly on the continental shelf during the MWP-1A. Furthermore, between 9.5 and 8.5 ka, Tjallingii et al. (2010) found a rapid migration of the Paleo-Mekong River mouth which was influenced by the enhanced rate of sea-level rise (25 mm/yr) from 34 to 9 m below the modern sea level corresponding to the sea-level jump of the meltwater pulse 1C (MWP-1C). Nevertheless, sea-level fluctuations may not greatly impact terrigenous sediment variations of sediment cores that are close to their sources (e.g., Liu et al., 2010; Wan et al., 2015; Sang et al., 2019). In comparison with sea-level fluctuations in this region, no important variations of clay minerals, major elements, and Sr-Nd isotopic compositions at Core MD05-2896 are observed evidently during the MWP-1A and -1C (**Figures 3, 4**), suggesting that the sea-level change may not have strongly affected the terrigenous sediment variations of the studied core over the last 45 ka. In addition, clay mineral assemblage and Sr-Nd isotopic compositions of Holocene and Pleistocene samples at the core are located adjacently (**Figures 5, 7**), indicating no obvious change in sediment sources under the effect of sea-level change since the late Pleistocene. These suggest that sea-level fluctuations cannot alter the overall trend of terrigenous sediment input in this region, and it only causes a trivial influence on terrigenous sediment variations. These hypotheses are also suitable for investigations on clay mineralogy and

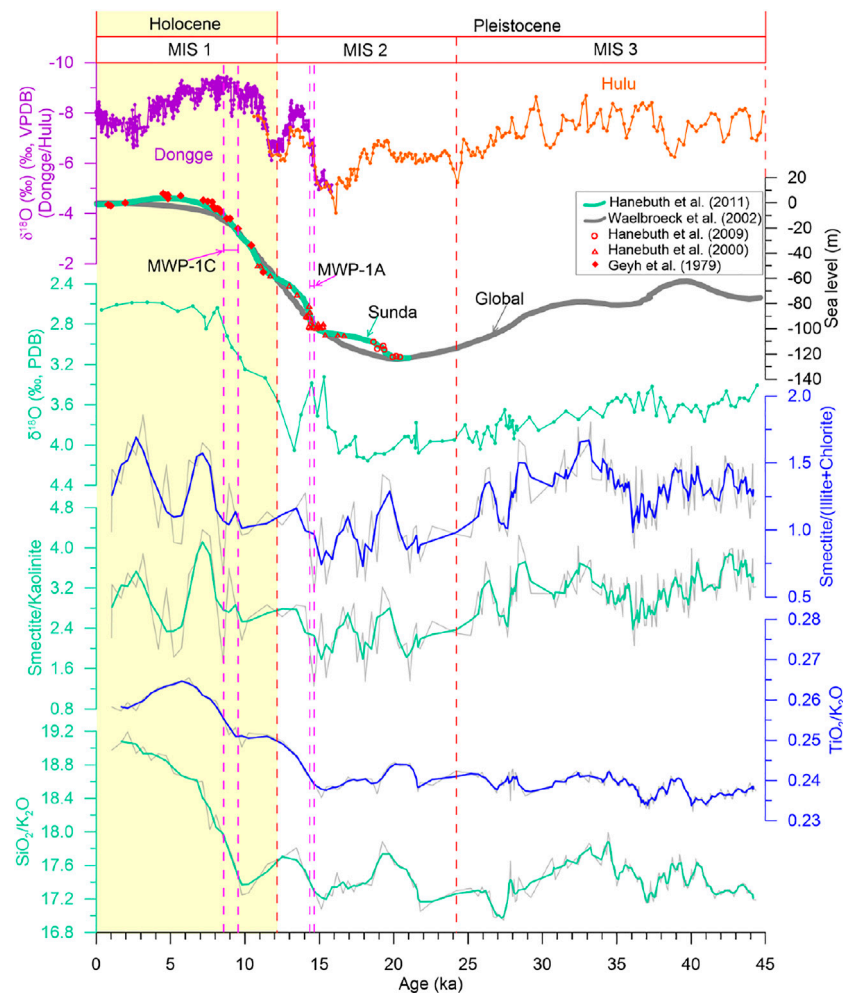


FIGURE 8 | Comparison of smectite/(illite + chlorite), smectite/kaolinite, $\text{SiO}_2/\text{K}_2\text{O}$, and $\text{TiO}_2/\text{K}_2\text{O}$ ratios of Core MD05-2896, with benthic foraminiferal *C. wuellerstorfi* $\delta^{18}\text{O}$ records at Core MD05-2896 (Wan et al., 2020) and stalagmite $\delta^{18}\text{O}$ records of the Hulu and Dongge Caves (Wang et al., 2001; Dykoski et al., 2005). Sea-level data are from Geyh et al. (1979), Waelbroeck et al. (2002), and Hanebuth et al. (2000); Hanebuth et al. (2009); Hanebuth et al. (2011). Dashed magenta lines indicate the meltwater pulses 1A (MWP-1A) (Hanebuth et al., 2000) and 1C (MWP-1C) (Tjallingii et al., 2010).

elemental geochemistry of Cores MD01-2393, MD97-2150, and SO18383-3 offshore from the Mekong River, which showed no apparent variations of terrigenous sediments under the impact of sea-level change during the MWP-1A and -1C (Liu et al., 2004; Liu et al., 2005; Colin et al., 2010; Jiwaringruengkul et al., 2019b). Undoubtedly, the Mekong River still contributes large terrigenous sediments to this region without any significant changes in sediment sources and terrigenous sediment variations under the influence of sea-level fluctuations over the last 45 ka.

5.3 Chemical Weathering and East Asian Monsoon Evolution

Based on the provenance analysis above, the Mekong River is the dominant source of terrigenous sediments to the Core MD05-2896. In addition, sea-level fluctuations could not have significantly impacted terrigenous sediment variations of this

core over the last 45 ka. This implies that terrigenous sediment variations of this core can relate intimately to the weathering processes in the source regions instead of sea-level changes in the southern South China Sea. Thus, clay minerals and major elements from this core can be used to investigate past changes in the chemical weathering intensity in the Mekong River basin. In Core MD05-2896, illite, chlorite, and kaolinite contents relatively present inverse correlations to smectite content (Figure 3), suggesting that they could be produced by different weathering processes in the Mekong River. In this basin, illite, chlorite, and kaolinite are derived from physical weathering and erosion, while smectite originates from chemical weathering. For these reasons, smectite/(illite + chlorite) and smectite/kaolinite ratios can be used as reasonable proxies for characterizing chemical weathering in the Mekong River basin (Figure 8). Thus, higher smectite/(illite + chlorite) and smectite/kaolinite ratios indicate enhanced intensive chemical weathering

conditions, whereas lower ratios represent the weakened intensity of chemical weathering conditions.

In the source regions, the chemical weathering of the parent rocks generally motivates the enrichment of immobile elements (e.g., Al, Si, Ti, and Fe) and movement of mobile elements (e.g., Ca, Na, K, and Mg) in weathering products (Nesbitt et al., 1980) and their behavior can be conserved in terrigenous sediments in the sea (Clift et al., 2014; Liu et al., 2016). Based on the behavior of major elements during the chemical weathering on the Earth's surface, the chemical index of alteration (CIA) (Nesbitt and Young, 1982), the weathering index of parker (WIP) (Parker, 1970), the plagioclase index of alteration (PIA) (Fedo et al., 1995), the index of compositional variability (CIW) (Harnois, 1988), A-CN-K and A-CN-K-FM ternary diagrams (Nesbitt and Young, 1984; Nesbitt and Young, 1989), and their oxide ratios (e.g., $\text{Al}_2\text{O}_3/\text{K}_2\text{O}$, $\text{SiO}_2/\text{K}_2\text{O}$, $\text{TiO}_2/\text{K}_2\text{O}$) have been widely utilized to identify the altered pathway and to evaluate the intensive chemical weathering in the source regions (e.g., Liu et al., 2004; Clift et al., 2014; Wan et al., 2015; Jiwrungrueangkul et al., 2019b; Sang et al., 2019). Nevertheless, the geochemical compositions of fluvial sediments are controlled by complex factors such as provenance geology, weathering and erosion processes, and hydrodynamic sorting (McLennan, 1993; Nesbitt et al., 1996; Garzanti and Resentini, 2016; Guo et al., 2018). Furthermore, the fluvial sediments in the large catchments may not be derived directly from the weathering of igneous rocks (i.e., first cycle) instead of recycled sedimentary rocks (Dellinger et al., 2014; Garzanti and Resentini, 2016). These imply that these weathering indices may reflect the integrated weathering history rather than the instantaneous weathering condition at the time of source-to-sink transport processes of fluvial sediments and these indices should be applied carefully to investigate the weathering history in a specific catchment. Examining **Figure 4**, variations in Al_2O_3 , Fe_2O_3 , TiO_2 , and SiO_2 contents don't display similar patterns over the last 45 ka, and variations in Na_2O , K_2O , CaO , and MgO contents also show different trends during MIS 3, 2, and 1. This may indicate that not all of these elemental oxide variations at this studied core relate significantly to the intensity of chemical weathering in this basin. Additionally, stronger physical erosion of inherited clays of ferrallitic soils in a lower part of the middle reach in the Mekong River basin could provide higher Al_2O_3 in fluvial sediments during MIS 2 than during MIS 3 and 1 (**Figure 4**). This event may impact CIA, WIP, PIA, and CIW values and Al_2O_3 /mobile element oxide ratios, indicating that these proxies could not display temporal changes in the intensive chemical weathering of the Mekong River basin over the last 45 ka.

In Core MD05-2896, variations in TiO_2 and SiO_2 contents inversely correlate to K_2O content (**Figure 4**), indicating that these elements relate to chemical weathering intensity in the Mekong River basin. SiO_2 and TiO_2 are relatively resistant to weathering (Nesbitt and Young, 1982; Wei et al., 2003), and they are mainly the terrigenous detrital origin of secondary minerals, including clay minerals in marine sediments (Zhang et al., 2002; Bastian et al., 2017). In contrast, K_2O is highly mobile during weathering processes, implying easy depletion in weathering products (Nesbitt et al., 1980; Condie et al., 1995). Based on the behavior of immobile elements (i.e., Si^{4+} and Ti^{4+}) and mobile

elements (i.e., K^+) during chemical weathering, $\text{SiO}_2/\text{K}_2\text{O}$ and $\text{TiO}_2/\text{K}_2\text{O}$ ratios can be used to reconstruct the intensity of chemical weathering in the source region. Variations in $\text{SiO}_2/\text{K}_2\text{O}$ and $\text{TiO}_2/\text{K}_2\text{O}$ ratios of Core MD05-2896 show similar changes over the last 45 ka (**Figure 8**), and an increase in these ratios indicates strengthened chemical weathering, while a decrease in the ratios suggests weakened chemical weathering.

During the last glacial MIS 3, the Mekong River basin is characterized by slightly strengthened chemical weathering, indicated by higher smectite/(illite + chlorite) (0.8–1.8) and smectite/kaolinite (2.0–4.2), but negligibly increased $\text{SiO}_2/\text{K}_2\text{O}$ (16.9–17.9) and $\text{TiO}_2/\text{K}_2\text{O}$ (0.2–0.24) ratios. Variations in these weathering proxies display a correspondence with benthic foraminiferal *C. wuellerstorfi* $\delta^{18}\text{O}$ records at Core MD05-2896 (Wan et al., 2020) and the stalagmite $\delta^{18}\text{O}$ records of Hulu Cave (Wang et al., 2001). After this period, the mineralogical proxies displayed evidently lower values, whereas the elemental ratios displayed unclear decreased values, implying that the degree of chemical weathering between the last glacial MIS 3 and MIS 2 are the unobvious difference and the clay mineralogical proxies may be more sensitive with variations in intensive chemical weathering than the elemental proxies.

During the last glacial MIS 2, the lowest values of 0.5–1.4 smectite/(illite + chlorite) and 1.2–3.2 smectite/kaolinite ratios, while no distinct decreased 17.0–17.8 $\text{SiO}_2/\text{K}_2\text{O}$ and 0.23–0.24 $\text{TiO}_2/\text{K}_2\text{O}$ ratios indicated the weakest chemical weathering in the Mekong River basin. $\text{SiO}_2/\text{K}_2\text{O}$ and $\text{TiO}_2/\text{K}_2\text{O}$ ratios during this period displayed trivial lower values than the last glacial MIS 3, implying no significant weakened chemical weathering during this period. Owing to the geochemistry of K being complicated, it is enriched in weathering products under moderate chemical weathering of the parent rocks in the source regions, while depleted under more intensive chemical weathering (Balxland, 1974; Condie et al., 1995; Nesbitt et al., 1980; Nesbitt et al., 1997). The decrease in chemical weathering correlates well to a weak monsoon intensity during this period reaching maximum values in the benthic *C. wuellerstorfi* $\delta^{18}\text{O}$ records at Core MD05-2896 and the stalagmite $\delta^{18}\text{O}$ records of the Hulu Cave and the Dongge Cave (Dykoski et al., 2005). At the end of this period, the mineralogical and elemental proxies displayed increased trends, suggesting enhanced chemical weathering in the source region with higher smectite and immobile elements (i.e., Si, Ti) in weathering products, while less abundance of illite, chlorite, and kaolinite, as well as stronger leaching of mobile elements (i.e., K).

During the Holocene (MIS 1), the East Asian monsoon displays strengthened summer monsoon and weakened winter monsoon, causing higher precipitation and hot-warm temperature in the source regions (Wang et al., 2001; Dykoski et al., 2005). In the Mekong River basin, the climatic setting is significantly controlled by the East Asian monsoon (Webster, 1994; Chu and Wang, 2003), suggesting that this river basin could be characterized by hot and warm climate conditions during the Holocene. The Mekong River basin has experienced strengthened chemical weathering as indicated by the increasing 0.67–1.8 smectite/(illite + chlorite), 1.7–4.3 smectite/kaolinite, 17.2–19.2 $\text{SiO}_2/\text{K}_2\text{O}$, and 0.2–0.3 $\text{TiO}_2/\text{K}_2\text{O}$ ratios.

The mineralogical proxies (smectite/(illite + chlorite) and smectite/kaolinite) and the geochemical proxies ($\text{SiO}_2/\text{K}_2\text{O}$ and

TiO₂/K₂O) for chemical weathering characterization of Core MD05-2896 in the southern South China Sea are effective indicators for reconstructing the history of chemical weathering in the Mekong River basin and the relationship between weathering process and East Asian monsoon evolution (Figure 8). In general, the smectite/(illite + chlorite), smectite/kaolinite, SiO₂/K₂O, and TiO₂/K₂O ratios showed an evident cyclicity with higher values during the last glacial MIS 3 and the Holocene (MIS 1), while the lower values during the last glacial MIS 2. Variations in these mineralogical and geochemical proxies present a close correlation to the benthic *C. wuellerstorfi* δ¹⁸O records at Core MD05-2896 (Wan et al., 2020) and the stalagmite δ¹⁸O records of the Hulu Cave (Wang et al., 2001) and the Dongge Cave (Dykoski et al., 2005). These suggest that the chemical weathering in the Mekong River basin has been strongly forced by the East Asian monsoon evolution over the last 45 ka. The last glacial MIS 3 and the Holocene MIS 1 are characterized by warm and humid climatic conditions, which facilitate strengthened chemical weathering in the Mekong River basin, yielding more secondary clay minerals (i.e., smectite) and enrichment of immobile elements (i.e., Si, Ti) in weathering products. On the contrary, the last glacial MIS 2 corresponds to cold and dry climatic conditions, causing weakened chemical weathering with higher occurrences of primary clay minerals (i.e., illite, chlorite) and mobile elements (i.e., K) in weathering profiles. As the 7th largest river in the world and the largest river in Southeast Asia, the Mekong River transports huge amounts of terrigenous sediments to the South China Sea under the strong influence of the East Asian monsoon. In this basin, source-to-sink transport processes of fluvial sediments highly relate to the weathering process and monsoon evolution. This study revealed the chemical weathering in the Mekong River basin and its relationship with the East Asian monsoon during the late Quaternary that can boost our understanding of the Earth's surface and monsoon evolution as well as the complex interaction between continental chemical weathering and climatic conditions globally, especially in South China and Southeast Asia regions.

6 CONCLUSION

Clay mineralogy, major-element geochemistry, and Sr-Nd isotopic compositions of Core MD05-2896 are employed to study the discrimination of sediment provenance in the southern South China Sea and to reconstruct a history of chemical weathering in the Mekong River basin over the last 45 ka. The research conclusions are as follows:

- 1) The clay mineral assemblage of Core MD05-2896 contains predominant smectite (27%–56%) and illite (18%–32%), with moderate kaolinite (13%–23%) and chlorite (11%–18%). ⁸⁷Sr/⁸⁶Sr ratios and ε_{Nd} values of Core MD05-2896 narrowly vary from 0.7232 to 0.7272 (average 0.7250) and from –10.9 to –9.6 (average –10.4), respectively.
- 2) Clay mineralogy and Sr-Nd isotopic composition results indicate that the Mekong River is the primary terrigenous sediment source supplying to the southern South China Sea with no obvious change in sediment sources, despite significant sea-level fluctuations over the last 45 ka.

- 3) Smectite/(illite + chlorite), smectite/kaolinite, SiO₂/K₂O, and TiO₂/K₂O ratios can be valuable proxies for reconstructing the history of chemical weathering in the Mekong River basin. An increase in smectite/(illite + chlorite), smectite/kaolinite, SiO₂/K₂O, and TiO₂/K₂O ratios indicates strengthened chemical weathering, whereas the decrease in these ratios suggests weakened chemical weathering. This study displays enhanced chemical weathering during the last glacial MIS 3 and the Holocene (MIS 1), while weakened chemical weathering during the last glacial MIS 2 in the Mekong River basin.
- 4) Variations in smectite/(illite + chlorite), smectite/kaolinite, SiO₂/K₂O, and TiO₂/K₂O ratios significantly relate to the climate records, implying that the chemical weathering history of the Mekong River basin is principally controlled by the East Asian monsoon evolution over the last 45 ka.

DATA AVAILABILITY STATEMENT

The original contributions presented in the study are included in the article/Supplementary Material; further inquiries can be directed to the corresponding authors.

AUTHOR CONTRIBUTIONS

PNS performed the experiments, analyzed and interpreted the data, and wrote the manuscript. ZL conceived and designed the experiments, analyzed and interpreted the data, contributed reagents, materials, analysis tools, or data, and wrote the manuscript. CC wrote the manuscript.

FUNDING

This work was supported by the National Key R&D Program of China (2018YFE0202400), the Second Tibetan Plateau Scientific Expedition and Research (STEP) Program (2019QZKK020403), and the Shanghai International Science and Technology Cooperation Fund (19230742100).

ACKNOWLEDGMENTS

The authors thank the crew and scientists on board the R/V Marion Dufresne for collecting the sediment core during the cruise IMAGES-MARCO POLO in 2005. They also thank Yanli li, Mingyang Yu, Hui Li, Juan Xu, and Pengfei Liu for laboratory assistance.

SUPPLEMENTARY MATERIAL

The Supplementary Material for this article can be found online at: <https://www.frontiersin.org/articles/10.3389/feart.2022.885547/full#supplementary-material>

REFERENCES

- Barber, A. J., and Crow, M. J. (2009). Structure of Sumatra and its Implications for the Tectonic Assembly of Southeast Asia and the Destruction of Paleotethys. *Isl. Arc* 18, 3–20. doi:10.1111/j.1440-1738.2008.00631.x
- Bastian, L., Revel, M., Bayon, G., Dufour, A., and Vigier, N. (2017). Abrupt Response of Chemical Weathering to Late Quaternary Hydroclimate Changes in Northeast Africa. *Sci. Rep.* 7, 44231. doi:10.1038/srep44231
- Beaulieu, E., Godd ris, Y., Donnadi u, Y., Labat, D., and Roelandt, C. (2012). High Sensitivity of the Continental-Weathering Carbon Dioxide Sink to Future Climate Change. *Nat. Clim. Change* 2, 346–349. doi:10.1038/nclimate1419
- Beny, F., Toucanne, S., Skonieczny, C., Bayon, G., and Ziegler, M. (2018). Geochemical Provenance of Sediments from the Northern East China Sea Document a Gradual Migration of the Asian Monsoon Belt over the Past 400,000 Years. *Quat. Sci. Rev.* 190, 161–175. doi:10.1016/j.quascirev.2018.04.032
- Berner, R. A., Lasaga, A. C., and Garrels, R. M. (1983). The Carbonate-Silicate Geochemical Cycle and its Effect on Atmospheric Carbon Dioxide over the Past 100 Million Years. *Am. J. Sci.* 283, 641–683. doi:10.2475/ajs.283.7.641
- Blandland, A. B. (1974). Geochemistry and Geochronology of Chemical Weathering, Butler Hill Granite, Missouri. *Geochimica Cosmochimica Acta* 38, 843–852. doi:10.1016/0016-7037(74)90059-3
- Boulay, S., Colin, C., Trentesaux, A., Clain, S., Liu, Z., and Lauer-Leredde, C. (2007). Sedimentary Responses to the Pleistocene Climatic Variations Recorded in the South China Sea. *Quat. Res.* 68, 162–172. doi:10.1016/j.yqres.2007.03.004
- Cai, G., Li, S., Zhao, L., Zhong, L., and Chen, H. (2020). Clay Minerals, Sr-Nd Isotopes and Provenance of Sediments in the Northwestern South China Sea. *J. Asian Earth Sci.* 202, 104531. doi:10.1016/j.jseas.2020.104531
- Chamley, H. (1989). *Clay Sedimentology*. New York: Springer. doi:10.1007/978-3-642-85916-8
- Chen, Q., Liu, Z., and Kissel, C. (2017). Clay Mineralogical and Geochemical Proxies of the East Asian Summer Monsoon Evolution in the South China Sea during Late Quaternary. *Sci. Rep.* 7, 1–9. doi:10.1038/srep42083
- Chesner, C. A. (2012). The Toba Caldera Complex. *Quat. Int.* 258, 5–18. doi:10.1016/j.quaint.2011.09.025
- Chu, P. C., and Wang, G. (2003). Seasonal Variability of Thermohaline Front in the Central South China Sea. *J. Oceanogr.* 59, 65–78. doi:10.1023/A:1022868407012
- Clift, P. D., Blusztajn, J., and Duc, N. A. (2006). Large-scale Drainage Capture and Surface Uplift in Eastern Tibet-SW China before 24 Ma Inferred from Sediments of the Hanoi Basin, Vietnam. *Geophys. Res. Lett.* 33, 1–5. doi:10.1029/2006gl027772
- Clift, P. D., Kulhanek, D. K., Zhou, P., Bowen, M. G., Vincent, S. M., Lyle, M., et al. (2020). Chemical Weathering and Erosion Responses to Changing Monsoon Climate in the Late Miocene of Southwest Asia. *Geol. Mag.* 157, 939–955. doi:10.1017/s0016756819000608
- Clift, P. D., Lee, J. I., Clark, M. K., and Blusztajn, J. (2002). Erosional Response of South China to Arc Rifting and Monsoonal Strengthening: A Record from the South China Sea. *Mar. Geol.* 184, 207–226. doi:10.1016/S0025-3227(01)00301-2
- Clift, P. D., Wan, S., and Blusztajn, J. (2014). Reconstructing Chemical Weathering, Physical Erosion and Monsoon Intensity since 25Ma in the Northern South China Sea: A Review of Competing Proxies. *Earth-Science Rev.* 130, 86–102. doi:10.1016/j.earscirev.2014.01.002
- Colin, C., Siani, G., Sicre, M.-A., and Liu, Z. (2010). Impact of the East Asian Monsoon Rainfall Changes on the Erosion of the Mekong River Basin over the Past 25,000yr. *Mar. Geol.* 271, 84–92. doi:10.1016/j.margeo.2010.01.013
- Colin, C., Turpin, L., Bertaux, J., Desprairies, A., and Kissel, C. (1999). Erosional History of the Himalayan and Burman Ranges during the Last Two Glacial-Interglacial Cycles. *Earth Planet. Sci. Lett.* 171, 647–660. doi:10.1016/S0012-821X(99)00184-3
- Colin, C., Turpin, L., Blamart, D., Frank, N., Kissel, C., and Duchamp, S. (2006). Evolution of Weathering Patterns in the Indo-Burman Ranges over the Last 280 Kyr: Effects of Sediment Sources on ⁸⁷Sr/⁸⁶Sr Ratios Tracer. *Geochem. Geophys. Geosyst.* 7, 1–16. doi:10.1029/2005gc000962
- Condie, K. C., Dengate, J., and Cullers, R. L. (1995). Behavior of Rare Earth Elements in a Paleoweathering Profile on Granodiorite in the Front Range, Colorado, USA. *Geochimica Cosmochimica Acta* 59, 279–294. doi:10.1016/0016-7037(94)00280-Y
- Conley, D. J. (2002). Terrestrial Ecosystems and the Global Biogeochemical Silica Cycle. *Glob. Biogeochem. Cycles*. 16, 1–8. doi:10.1029/2002gb001894
- Dellinger, M., Gaillardet, J., Bouchez, J., Calmels, D., Galy, V., Hilton, R. G., et al. (2014). Lithium Isotopes in Large Rivers Reveal the Cannibalistic Nature of Modern Continental Weathering and Erosion. *Earth Planet. Sci. Lett.* 401, 359–372. doi:10.1016/j.epsl.2014.05.061
- Dykoski, C., Edwards, R., Cheng, H., Yuan, D., Cai, Y., Zhang, M., et al. (2005). A High-Resolution, Absolute-Dated Holocene and Deglacial Asian Monsoon Record from Dongge Cave, China. *Earth Planet. Sci. Lett.* 233, 71–86. doi:10.1016/j.epsl.2005.01.036
- Ehrmann, W. (1998). Implications of Late Eocene to Early Miocene Clay Mineral Assemblages in McMurdo Sound (Ross Sea, Antarctica) on Paleoclimate and Ice Dynamics. *Palaeogeogr. Palaeoclimatol. Palaeoecol.* 139, 213–231. doi:10.1016/S0031-0182(97)00138-7
- Esquevin, J. (1969). Influence de la composition chimique des illites surcristallinite. *Bull. Cent. Rech. Rau-SNP A* 3, 147–153.
- Fedo, C. M., Wayne Nesbitt, H., and Young, G. M. (1995). Unraveling the Effects of Potassium Metasomatism in Sedimentary Rocks and Paleosols, with Implications for Paleoweathering Conditions and Provenance. *Geol.* 23, 921–924. doi:10.1130/0091-7613(1995)023<0921:uteopm>2.3.co;2
- Garzanti, E., and Resentini, A. (2016). Provenance Control on Chemical Indices of Weathering (Taiwan River Sands). *Sediment. Geol.* 336, 81–95. doi:10.1016/j.sedgeo.2015.06.013
- Geyh, M. A., Streif, H., and Kudrass, H.-R. (1979). Sea-level Changes during the Late Pleistocene and Holocene in the Strait of Malacca. *Nature* 278, 441–443. doi:10.1038/278441a0
- Gibbs, R. J. (1977). Clay Mineral Segregation in the Marine Environment. *J. Sediment. Res.* 47, 237–243. doi:10.1306/212f713a-2b24-11d7-8648000102c1865d
- Gingele, F. X., M ller, P. M., and Schneider, R. R. (1998). Orbital Forcing of Freshwater Input in the Zaire Fan Area-Clay Mineral Evidence from the Last 200 Kyr. *Palaeogeogr. Palaeoclimatol. Palaeoecol.* 138, 17–26. doi:10.1016/S0031-0182(97)00121-1
- Guo, Y., Yang, S., Su, N., Li, C., Yin, P., and Wang, Z. (2018). Revisiting the Effects of Hydrodynamic Sorting and Sedimentary Recycling on Chemical Weathering Indices. *Geochimica Cosmochimica Acta* 227, 48–63. doi:10.1016/j.gca.2018.02.015
- Hall, R. (2002). Cenozoic Geological and Plate Tectonic Evolution of SE Asia and the SW Pacific: Computer-Based Reconstructions, Model and Animations. *J. Asian Earth Sci.* 20, 353–431. doi:10.1016/S1367-9120(01)00069-4
- Hanebuth, T. J. J., Statterger, K., and Bojanowski, A. (2009). Termination of the Last Glacial Maximum Sea-Level Lowstand: The Sunda-Shelf Data Revisited. *Glob. Planet. Change* 66, 76–84. doi:10.1016/j.gloplacha.2008.03.011
- Hanebuth, T. J. J., Voris, H. K., Yokoyama, Y., Saito, Y., and Okuno, J. i. (2011). Formation and Fate of Sedimentary Depocentres on Southeast Asia's Sunda Shelf over the Past Sea-Level Cycle and Biogeographic Implications. *Earth-Science Rev.* 104, 92–110. doi:10.1016/j.earscirev.2010.09.006
- Hanebuth, T., Statterger, K., and Grootes, P. M. (2000). Rapid Flooding of the Sunda Shelf: A Late-Glacial Sea-Level Record. *Science* 288, 1033–1035. doi:10.1126/science.288.5468.1033
- Hanebuth, T., Statterger, K., and Saito, Y. (2002). The Stratigraphic Architecture of the Central Sunda Shelf (SE Asia) Recorded by Shallow-Seismic Surveying. *Geo-Marine Lett.* 22, 86–94. doi:10.1007/s00367-002-0102-1
- Harnois, L. (1988). The CIW Index: A New Chemical Index of Weathering. *Sediment. Geol.* 55, 319–322. doi:10.1016/0037-0738(88)90137-6
- Holtzapffel, T. (1985). *Les min raux argileux: Pr paration, analyse diffractom trique et d termination*, 12. Lille: Society G ologique Nord Publication, 1–136.
- Hu, J., Peng, P. a., Fang, D., Jia, G., Jian, Z., and Wang, P. (2003). No Aridity in Sunda Land during the Last Glaciation: Evidence from Molecular-Isotopic Stratigraphy of Long-Chain N-Alkanes. *Palaeogeogr. Palaeoclimatol. Palaeoecol.* 201, 269–281. doi:10.1016/S0031-0182(03)00613-8
- Huang, J., Jiang, F., Wan, S., Zhang, J., Li, A., and Li, T. (2016). Terrigenous Supplies Variability over the Past 22,000yr in the Southern South China Sea Slope: Relation to Sea Level and Monsoon Rainfall Changes. *J. Asian Earth Sci.* 117, 317–327. doi:10.1016/j.jseas.2015.12.019

- Hutchison, C. S. (1968). Dating Tectonism in the Indosinian-Thai-Malayan Orogen by Thermoluminescence. *Geol. Soc. Am. Bull.* 79, 375–386. doi:10.1130/0016-7606(1968)79[375:dtitio]2.0.co;2
- Hutchison, C. S. (2005). *Geology of North-West Borneo: Sarawak, Brunei and Sabah*. Amsterdam: Elsevier Science.
- Innocent, C., Fagel, N., and Hillaire-Marcel, C. (2000). Sm-Nd Isotope Systematics in Deep-Sea Sediments: Clay-size versus Coarser Fractions. *Mar. Geol.* 168, 79–87. doi:10.1016/S0025-3227(00)00052-9
- Jacobsen, S. B., and Wasserburg, G. J. (1980). Sm-Nd Isotopic Evolution of Chondrites. *Earth Planet. Sci. Lett.* 50, 139–155. doi:10.1016/0012-821X(80)90125-9
- Jiwarungueangkul, T., Liu, Z., Statterger, K., and Sang, P. N. (2019b). Reconstructing Chemical Weathering Intensity in the Mekong River Basin since the Last Glacial Maximum. *Paleoceanogr. Paleoclimatology* 34, 1710–1725. doi:10.1029/2019pa003608
- Jiwarungueangkul, T., Liu, Z., and Zhao, Y. (2019a). Terrigenous Sediment Input Responding to Sea Level Change and East Asian Monsoon Evolution since the Last Deglaciation in the Southern South China Sea. *Glob. Planet. Change* 174, 127–137. doi:10.1016/j.gloplacha.2019.01.011
- Johnson, A. G., and Kelley, J. T. (1984). Temporal, Spatial, and Textural Variation in the Mineralogy of Mississippi River Suspended Sediment. *J. Sediment. Res.* 54, 67–72. doi:10.1306/212f83a5-2b24-11d7-8648000102c1865d
- Krumm, S., and Buggisch, W. (1991). Sample Preparation Effects on Illite Crystallinity Measurement: Grain-Size Gradation and Particle Orientation. *J. Metamorph. Geol.* 9, 671–677. doi:10.1111/j.1525-1314.1991.tb00557.x
- Lai, Y. M., Chung, S. L., Ghani, A. A., Murtadha, S., Lee, H. Y., and Chu, M. F. (2021). Mid-Miocene Volcanic Migration in the Westernmost Sunda Arc Induced by India-Eurasia Collision. *Geology*. 49, 713–717. doi:10.1130/g48568.1
- Laj, C., Wang, P. X., Balut, Y., and Al, E. (2005). *MD147-Marco Polo Images XII Cruise Report*. Brest: Institut Polaire Français, 149.
- Liu, Z., Colin, C., Huang, W., Phon Le, K., Tong, S., Chen, Z., et al. (2007a). Climatic and Tectonic Controls on Weathering in South China and Indochina Peninsula: Clay Mineralogical and Geochemical Investigations from the Pearl, Red, and Mekong Drainage Basins. *Geochem. Geophys. Geosyst.* 8, 1–18. doi:10.1029/2006gc001490
- Liu, Z., Colin, C., Li, X., Zhao, Y., Tuo, S., Chen, Z., et al. (2010). Clay Mineral Distribution in Surface Sediments of the Northeastern South China Sea and Surrounding Fluvial Drainage Basins: Source and Transport. *Mar. Geol.* 277, 48–60. doi:10.1016/j.margeo.2010.08.010
- Liu, Z., Colin, C., Trentesaux, A., Blamart, D., Bassinot, F., Siani, G., et al. (2004). Erosional History of the Eastern Tibetan Plateau since 190 Kyr Ago: Clay Mineralogical and Geochemical Investigations from the Southwestern South China Sea. *Mar. Geol.* 209, 1–18. doi:10.1016/j.margeo.2004.06.004
- Liu, Z., Colin, C., Trentesaux, A., Siani, G., Frank, N., Blamart, D., et al. (2005). Late Quaternary Climatic Control on Erosion and Weathering in the Eastern Tibetan Plateau and the Mekong Basin. *Quat. Res.* 63, 316–328. doi:10.1016/j.yqres.2005.02.005
- Liu, Z., and Statterger, K. (2014). South China Sea Fluvial Sediments: An Introduction. *J. Asian Earth Sci.* 79, 507–508. doi:10.1016/j.jseas.2013.11.003
- Liu, Z., Trentesaux, A., Clemens, S. C., Colin, C., Wang, P., Huang, B., et al. (2003). Clay Mineral Assemblages in the Northern South China Sea: Implications for East Asian Monsoon Evolution over the Past 2 Million Years. *Mar. Geol.* 201, 133–146. doi:10.1016/S0025-3227(03)00213-5
- Liu, Z., Tuo, S., Colin, C., Liu, J. T., Huang, C.-Y., Selvaraj, K., et al. (2008). Detrital Fine-Grained Sediment Contribution from Taiwan to the Northern South China Sea and its Relation to Regional Ocean Circulation. *Mar. Geol.* 255, 149–155. doi:10.1016/j.margeo.2008.08.003
- Liu, Z., Wang, H., Hantoro, W. S., Sathiamurthy, E., Colin, C., Zhao, Y., et al. (2012). Climatic and Tectonic Controls on Chemical Weathering in Tropical Southeast Asia (Malay Peninsula, Borneo, and Sumatra). *Chem. Geol.* 291, 1–12. doi:10.1016/j.chemgeo.2011.11.015
- Liu, Z., Zhao, Y., Colin, C., Statterger, K., Wiesner, M. G., Huh, C.-A., et al. (2016). Source-to-sink Transport Processes of Fluvial Sediments in the South China Sea. *Earth-Science Rev.* 153, 238–273. doi:10.1016/j.earscirev.2015.08.005
- Liu, Z., Zhao, Y., Li, J., and Colin, C. (2007b). Late Quaternary Clay Minerals off Middle Vietnam in the Western South China Sea: Implications for Source Analysis and East Asian Monsoon Evolution. *Sci. China Ser. D.* 50, 1674–1684. doi:10.1007/s11430-007-0115-8
- Lugmair, G. W., Shimamura, T., Lewis, R. S., and Anders, E. (1983). Samarium-146 in the Early Solar System: Evidence from Neodymium in the Allende Meteorite. *Science* 222, 1015–1018. doi:10.1126/science.222.4627.1015
- Lupker, M., France-Lanord, C., Galy, V., Lavé, J., and Kudrass, H. (2013). Increasing Chemical Weathering in the Himalayan System since the Last Glacial Maximum. *Earth Planet. Sci. Lett.* 365, 243–252. doi:10.1016/j.epsl.2013.01.038
- Martinson, D. G., Pisias, N. G., Hays, J. D., Imbrie, J., Moore, T. C., and Shackleton, N. J. (1987). Age Dating and the Orbital Theory of the Ice Ages: Development of a High-Resolution 0 to 300,000-Year Chronostratigraphy. *Quat. Res.* 27, 1–29. doi:10.1016/0033-5894(87)90046-9
- McLennan, S. M., and Hemming, S. (1992). Samarium/neodymium Elemental and Isotopic Systematics in Sedimentary Rocks. *Geochimica Cosmochimica Acta* 56, 887–898. doi:10.1016/0016-7037(92)90034-G
- McLennan, S. M., Taylor, S. R., Mcculloch, M. T., and Maynard, J. B. (1990). Geochemical and NdSr Isotopic Composition of Deep-Sea Turbidites: Crustal Evolution and Plate Tectonic Associations. *Geochimica Cosmochimica Acta* 54, 2015–2050. doi:10.1016/0016-7037(90)90269-Q
- McLennan, S. M. (1993). Weathering and Global Denudation. *J. Geol.* 101, 295–303. doi:10.1086/648222
- Meybeck, M. (1982). Carbon, Nitrogen, and Phosphorus Transport by World Rivers. *Am. J. Sci.* 282, 401–450. doi:10.2475/ajs.282.4.401
- Milliman, J. D., and Farnsworth, K. L. (2011). *River Discharge to the Coastal Ocean: A Global Synthesis*. Cambridge: Cambridge University Press. doi:10.5670/oceanog.2011.108
- Milliman, J. D., and Syvitski, J. P. M. (1992). Geomorphic/tectonic Control of Sediment Discharge to the Ocean: The Importance of Small Mountainous Rivers. *J. Geol.* 100, 525–544. doi:10.1086/629606
- Nesbitt, H. W., Fedo, C. M., and Young, G. M. (1997). Quartz and Feldspar Stability, Steady and Non-Steady-State Weathering, and Petrogenesis of Siliciclastic Sands and Muds. *J. Geol.* 105, 173–192. doi:10.1086/515908
- Nesbitt, H. W., Markovics, G., and Price, R. C. (1980). Chemical Processes Affecting Alkalis and Alkaline Earths during Continental Weathering. *Geochimica Cosmochimica Acta* 44, 1659–1666. doi:10.1016/0016-7037(80)90218-5
- Nesbitt, H. W., and Young, G. M. (1982). Early Proterozoic Climates and Plate Motions Inferred from Major Element Chemistry of Lutites. *Nature* 299, 715–717. doi:10.1038/299715a0
- Nesbitt, H. W., and Young, G. M. (1989). Formation and Diagenesis of Weathering Profiles. *J. Geol.* 97, 129–147. doi:10.1086/629290
- Nesbitt, H. W., Young, G. M., McLennan, S. M., and Keays, R. R. (1996). Effects of Chemical Weathering and Sorting on the Petrogenesis of Siliciclastic Sediments, with Implications for Provenance Studies. *J. Geol.* 104, 525–542. doi:10.1086/629850
- Nesbitt, H. W., and Young, G. M. (1984). Prediction of Some Weathering Trends of Plutonic and Volcanic Rocks Based on Thermodynamic and Kinetic Considerations. *Geochimica Cosmochimica Acta* 48, 1523–1534. doi:10.1016/0016-7037(84)90408-3
- Parker, A. (1970). An Index of Weathering for Silicate Rocks. *Geol. Mag.* 107, 501–504. doi:10.1017/S0016756800058581
- Patchineelam, S. M., and de Figueiredo, A. G. (2000). Preferential Settling of Smeectite on the Amazon Continental Shelf. *Geo-Marine Lett.* 20, 37–42. doi:10.1007/s003670000035
- Petschick, R. (2000). *MacDiff 4.2.2 [online]*. Available at <http://servermac.geologie.unfrankfurt.de/Rainr.html> (cited 12 1, 2001).[-
- Qin, J., Huh, Y., Edmond, J. M., Du, G., and Ran, J. (2006). Chemical and Physical Weathering in the Min Jiang, a Headwater Tributary of the Yangtze River. *Chem. Geol.* 227, 53–69. doi:10.1016/j.chemgeo.2005.09.011
- Rangin, C., Bellon, H., Benard, F., Letouzey, J., Muller, C., and Sanudin, T. (1990). Neogene Arc-Continent Collision in Sabah, Northern Borneo (Malaysia). *Tectonophysics* 183, 305–319. doi:10.1016/0040-1951(90)90423-6
- Revel, M., Sinko, J. A., Grousset, F. E., and Biscaye, P. E. (1996). Sr and Nd Isotopes as Tracers of North Atlantic Lithic Particles: Paleoclimatic Implications. *Paleoceanography* 11, 95–113. doi:10.1029/95pa03199
- Sang, P. N., Liu, Z., and Statterger, K. (2019). Weathering and Erosion in Central Vietnam over the Holocene and Younger Dryas: Clay Mineralogy and Elemental Geochemistry from the Vietnam Shelf, Western South China Sea. *J. Asian Earth Sci.* 179, 1–10. doi:10.1016/j.jseas.2019.04.008

- Sang, P. N., and Liu, Z. (2021). Terrigenous Sediment Variations in the Western South China Sea and Their Implications to East Asian Monsoon Evolution during the Last Glacial-Interglacial Cycle. *Quat. Int.* 580, 1–10. doi:10.1016/j.quaint.2021.02.008
- Sathiamurthy, E., and Voris, K. H. (2006). Maps of Holocene Sea Level Transgression and Submerged Lakes on the Sunda Shelf. *Trop. Nat. Hist.* 2, 1–44.
- Schimanski, A., and Statterger, K. (2005). Deglacial and Holocene Evolution of the Vietnam Shelf: Stratigraphy, Sediments and Sea-Level Change. *Mar. Geol.* 214, 365–387. doi:10.1016/j.margeo.2004.11.001
- Segalen, P. (1995). *Les Sols Ferrallitiques Et Leur Repartition Geographique*. Tome 3. Paris: editions De l'Orstom, Collection des Etudes et Theses.
- Steinke, S., Hanebuth, T. J. J., Vogt, C., and Statterger, K. (2008). Sea Level Induced Variations in Clay Mineral Composition in the Southwestern South China Sea over the Past 17,000 Yr. *Mar. Geol.* 250, 199–210. doi:10.1016/j.margeo.2008.01.005
- Sultan, K., and Shazili, N. A. (2009). Distribution and Geochemical Baselines of Major, Minor and Trace Elements in Tropical Topsoils of the Terengganu River Basin, Malaysia. *J. Geochem. Explor.* 103, 57–68. doi:10.1016/j.gexplo.2009.07.001
- Sun, X., Li, X., and Luo, Y. (2002). Vegetation and Climate on the Sunda Shelf of the South China Sea during the Last Glaciation-Pollen Results from Station 17962. *Acta Bot. Sin.* 44, 746–752.
- Tamburini, F., Adatte, T., Föllmi, K., Bernasconi, S. M., and Steinmann, P. (2003). Investigating the History of East Asian Monsoon and Climate during the Last Glacial-Interglacial Period (0–140 000 years): Mineralogy and Geochemistry of ODP Sites 1143 and 1144, South China Sea. *Mar. Geol.* 201, 147–168. doi:10.1016/S0025-3227(03)00214-7
- Tanaka, T., Togashi, S., Kamioka, H., Amakawa, H., Kagami, H., Hamamoto, T., et al. (2000). JNdI-1: A Neodymium Isotopic Reference in Consistency with LaJolla Neodymium. *Chem. Geol.* 168, 279–281. doi:10.1016/S0009-2541(00)00198-4
- Tjallingii, R., Statterger, K., Stocchi, P., Saito, Y., and Wetzel, A. (2014). Rapid Flooding of the Southern Vietnam Shelf during the Early to Mid-holocene. *J. Quat. Sci.* 29, 581–588. doi:10.1002/jqs.2731
- Tjallingii, R., Statterger, K., Wetzel, A., and Van Phach, P. (2010). Infilling and Flooding of the Mekong River Incised Valley during Deglacial Sea-Level Rise. *Quat. Sci. Rev.* 29, 1432–1444. doi:10.1016/j.quascirev.2010.02.022
- Voris, H. K. (2000). Maps of Pleistocene Sea Levels in Southeast Asia: Shorelines, River Systems and Time Durations. *J. Biogeogr.* 27, 1153–1167. doi:10.1046/j.1365-2699.2000.00489.x
- Waelbroeck, C., Labeyrie, L., Michel, E., Duplessy, J. C., McManus, J. F., Lambeck, K., et al. (2002). Sea-level and Deep Water Temperature Changes Derived from Benthic Foraminifera Isotopic Records. *Quat. Sci. Rev.* 21, 295–305. doi:10.1016/S0277-3791(01)00101-9
- WalKer, J. C. G., Hays, P. B., and Kasting, J. F. (1981). A Negative Feedback Mechanism for the Long-Term Stabilization of Earth's Surface Temperature. *J. Geophys. Res.* 86, 9776–9782. doi:10.1029/jc086ic10p09776
- Walter, H. J., Hegner, E., Diekmann, B., Kuhn, G., and Rutgers Van Der Loeff, M. M. (2000). Provenance and Transport of Terrigenous Sediment in the South Atlantic Ocean and Their Relations to Glacial and Interglacial Cycles: Nd and Sr Isotopic Evidence. *Geochimica Cosmochimica Acta* 64, 3813–3827. doi:10.1016/S0016-7037(00)00476-2
- Wan, S., Clift, P. D., Zhao, D., Hovius, N., Munhoven, G., France-Lanord, C., et al. (2017). Enhanced Silicate Weathering of Tropical Shelf Sediments Exposed during Glacial Lowstands: A Sink for Atmospheric CO₂. *Geochimica Cosmochimica Acta* 200, 123–144. doi:10.1016/j.gca.2016.12.010
- Wan, S., and Jian, Z. (2014). Deep Water Exchanges between the South China Sea and the Pacific since the Last Glacial Period. *Paleoceanography* 29, 1162–1178. doi:10.1002/2013pa002578
- Wan, S., Jian, Z., Gong, X., Dang, H., Wu, J., and Qiao, P. (2020). Deep Water [CO₃²⁻] and Circulation in the South China Sea over the Last Glacial Cycle. *Quat. Sci. Rev.* 243, 106499. doi:10.1016/j.quascirev.2020.106499
- Wan, S., Li, A., Clift, P. D., and Stuu, J.-B. W. (2007). Development of the East Asian Monsoon: Mineralogical and Sedimentological Records in the Northern South China Sea since 20 Ma. *Palaeogeogr. Palaeoclimatol. Palaeoecol.* 254, 561–582. doi:10.1016/j.palaeo.2007.07.009
- Wan, S., Toucanne, S., Clift, P. D., Zhao, D., Bayon, G., Yu, Z., et al. (2015). Human Impact Overwhelms Long-Term Climate Control of Weathering and Erosion in Southwest China. *Geology* 43, 439–442. doi:10.1130/g36570.1
- Wang, J., Li, A., Xu, K., Zheng, X., and Huang, J. (2015). Clay Mineral and Grain Size Studies of Sediment Provenances and Paleoenvironment Evolution in the Middle Okinawa Trough since 17ka. *Mar. Geol.* 366, 49–61. doi:10.1016/j.margeo.2015.04.007
- Wang, L., Sarnthein, M., Erlenkeuser, H., Grimalt, J., Grootes, P., Heilig, S., et al. (1999). East Asian Monsoon Climate during the Late Pleistocene: High-Resolution Sediment Records from the South China Sea. *Mar. Geol.* 156, 245–284. doi:10.1016/S0025-3227(98)00182-0
- Wang, P., Wang, L., Bian, Y., and Jian, Z. (1995). Late Quaternary Paleoceanography of the South China Sea: Surface Circulation and Carbonate Cycles. *Mar. Geol.* 127, 145–165. doi:10.1016/0025-3227(95)00008-M
- Wang, X., Sun, X., Wang, P., and Statterger, K. (2009). Vegetation on the Sunda Shelf, South China Sea, during the Last Glacial Maximum. *Palaeogeogr. Palaeoclimatol. Palaeoecol.* 278, 88–97. doi:10.1016/j.palaeo.2009.04.008
- Wang, Y. J., Cheng, H., Edwards, R. L., An, Z. S., Wu, J. Y., Shen, C. C., et al. (2001). A High-Resolution Absolute-Dated Late Pleistocene Monsoon Record from Hulu Cave, China. *Science* 294, 2345–2348. doi:10.1126/science.1064618
- Warrier, A. K., and Shankar, R. (2009). Geochemical Evidence for the Use of Magnetic Susceptibility as a Paleorainfall Proxy in the Tropics. *Chem. Geol.* 265, 553–562. doi:10.1016/j.chemgeo.2009.05.023
- Webster, P. J. (1994). The Role of Hydrological Processes in Ocean-Atmosphere Interactions. *Rev. Geophys.* 32, 427–476. doi:10.1029/94rg01873
- Wehausen, R., Tian, J., Brumsack, H. J., Cheng, X., and Wang, P. (2003). Geochemistry of Pliocene Sediments from ODP Site 1143 (Southern South China Sea). *Proc. Ocean Drill. Program. Sci. Results* 184, 1–25. doi:10.2973/odp.proc.sr.184.201.2003
- Wei, G., Liu, Y., Li, X., Shao, L., and Liang, X. (2003). Climatic Impact on Al, K, Sc and Ti in Marine Sediments: Evidence from ODP Site 1144, South China Sea. *Geochem. J.* 37, 593–602. doi:10.2343/geochemj.37.593
- Wei, G., Liu, Y., Ma, J., Xie, L., Chen, J., Deng, W., et al. (2012). Nd, Sr Isotopes and Elemental Geochemistry of Surface Sediments from the South China Sea: Implications for Provenance Tracing. *Mar. Geol.* 319–322, 21–34. doi:10.1016/j.margeo.2012.05.007
- Wu, J., Liu, Z., and Yu, X. (2021). Plagioclase-regulated Hydrothermal Alteration of Basaltic Rocks with Implications for the South China Sea Rifting. *Chem. Geol.* 585, 120569. doi:10.1016/j.chemgeo.2021.120569
- Wu, K., Shi, X., Lou, Z., Wu, B., Li, J., and Zhang, H. (2021). Sedimentary Responses to Climate Changes and Human Activities over the Past 7400 Years in the Western Sunda Shelf. *Front. Earth Sci.* 9, 1–16. doi:10.3389/feart.2021.631815
- Yan, Y., Carter, A., Palk, C., Bricchau, S., and Hu, X. (2011). Understanding Sedimentation in the Song Hong-Yinggehai Basin, South China Sea. *Geochem. Geophys. Geosyst.* 12, 1–15. doi:10.1029/2011gc003533
- Yang, S. Y., Jung, H. S., Lim, D. I., and Li, C. X. (2003). A Review on the Provenance Discrimination of Sediments in the Yellow Sea. *Earth-Science Rev.* 63, 93–120. doi:10.1016/S0012-8252(03)00033-3
- Zhang, C., Wang, L., Li, G., Dong, S., Yang, J., and Wang, X. (2002). Grain Size Effect on Multi-Element Concentrations in Sediments from the Intertidal Flats of Bohai Bay, China. *Appl. Geochem.* 17, 59–68. doi:10.1016/S0883-2927(01)00079-8
- Zhao, S., Liu, Z., Colin, C., Zhao, Y., Wang, X., and Jian, Z. (2018). Responses the East Asian Summer Monsoon in the Low-latitude South China Sea to High-latitude Millennial-scale Climatic Changes during the Last Glaciation: Evidence from a High-resolution Clay Mineralogical Record. *Paleoceanogr. Paleoclimatol.* 33, 1–20. doi:10.1029/2017pa003235

Conflict of Interest: The authors declare that the research was conducted in the absence of any commercial or financial relationships that could be construed as a potential conflict of interest.

Publisher's Note: All claims expressed in this article are solely those of the authors and do not necessarily represent those of their affiliated organizations, or those of the publisher, the editors, and the reviewers. Any product that may be evaluated in this article, or claim that may be made by its manufacturer, is not guaranteed or endorsed by the publisher.

Copyright © 2022 Sang, Liu and Colin. This is an open-access article distributed under the terms of the Creative Commons Attribution License (CC BY). The use, distribution or reproduction in other forums is permitted, provided the original author(s) and the copyright owner(s) are credited and that the original publication in this journal is cited, in accordance with accepted academic practice. No use, distribution or reproduction is permitted which does not comply with these terms.